Journal of Computational Physics, Volume 228, Issue 18, 1 October 2009, Pages 7046-7068

Accepted Manuscript

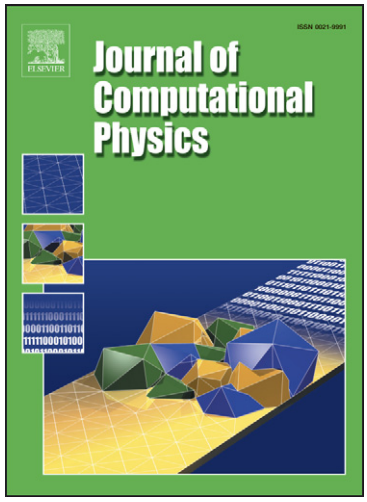

Exact and approximate solutions of Riemann problems in non-linear elasticity

P.T. Barton, D. Drikakis, E. Romenski, V.A. Titarev

PII: S0021-9991(09)00338-6
DOI: 10.1016/j.jcp.2009.06.014
Reference: YJCPH 2635

To appear in: *Journal of Computational Physics*

Received Date: 4 December 2008
Revised Date: 9 June 2009
Accepted Date: 18 June 2009

Please cite this article as: P.T. Barton, D. Drikakis, E. Romenski, V.A. Titarev, Exact and approximate solutions of Riemann problems in non-linear elasticity, *Journal of Computational Physics* (2009), doi: 10.1016/j.jcp.2009.06.014

Exact and approximate solutions of Riemann problems in non-linear elasticity

P.T. Barton[a], D. Drikakis[*,a], E. Romenski[a,1], V.A. Titarev[a]

[a] *Department of Aerospace Sciences, Cranfield University, Cranfield, Bedfordshire, MK43 0AL, UK*

Abstract

Eulerian shock-capturing schemes have advantages for modelling problems involving complex non-linear wave structures and large deformations in solid media. Various numerical methods now exist for solving hyperbolic conservation laws that have yet to be applied to non-linear elastic theory. In this paper one such class of solver is examined based upon characteristic tracing in conjunction with high-order monotonicity preserving weighted essentially non-oscillatory (MPWENO) reconstruction. Furthermore, a new iterative method for finding exact solutions of the Riemann problem in non-linear elasticity is presented. Access to exact solutions enables an assessment of the performance of the numerical techniques with focus on the resolution of the seven wave structure. The governing model represents a special case of a more general theory describing additional physics such as material plasticity. The numerical scheme therefore provides a firm basis for extension to simulate more complex physical phenomena. Comparison of exact and numerical solutions of one-dimensional initial values problems involving three-dimensional deformations is presented.

Key words: Riemann problem, WENO, solid mechanics, non-linear elasticity

1. Introduction

The Riemann problem is an initial value problem consisting of two uniform conditions where the state varies discontinuously. Depending on how these uniform states are chosen the Riemann problem for the equations of non-linear elasticity can result in up to six genuinely non-linear waves propagating away from a central linearly degenerate contact. Between each wave the state is uniform and hence the wavespeeds are constant, leading to a self similar profile of up to eight piecewise constant states.

Solution of the Riemann problem has gained significant importance in numerical schemes for systems of hyperbolic conservation laws. Considering a computational mesh with piecewise constant data stored at each discrete point, Godunov proposed solving Riemann problems locally at each intercell boundary. What has now become commonly known as the Godunov method permits numerical computation of more general Cauchy problems where discontinuities may exist in the solution. For such problems these shock-capturing schemes are popular since they avoid the need to explicitly include artificial viscosity to ensure convergence to the correct weak solution.

Here, the interest is in developing Godunov methods for solid media in the Eulerian reference frame. Although more complicated than Lagrangian schemes, Eulerian formulations are better suited for modelling problems involving discontinuous waves and large deformations. Several authors have proposed Eulerian schemes based on solving Riemann problems for solid materials. In [11, 24] approximate one-dimensional Riemann solvers are presented for two-dimensional deformations. Godunov methods for elastic-plastic media are demonstrated in [27, 29] for one-dimension, in [28] for two-dimensions, and in [13] for three dimensions.

The application of these numerical tools for solid mechanics is made possible by formulations of the governing laws as first order hyperbolic systems of conservation laws in the Eulerian reference frame. This

[*] d.drikakis@cranfield.ac.uk

[1] On leave from Sobolev Institute of Mathematics, Russian Academy of Sciences, Novosibirsk, Russia

is as opposed to the more traditional second order systems employed in elasticity. Here, the formulation proposed by Godunov and Romenski [8] is used, where the state of solid media is governed by conservation laws for mass, momentum, strain and energy, in conjunction with compatibility constraints (see also [17]). It should be mentioned that solution of the Riemann problem in non-linear elasticity is a stepping stone towards developing numerical schemes for elastic-plastic media. Indeed it is shown in [8, 19] that plasticity can be governed by the addition of higher terms and thus with no change to the Riemann solver employed for the convective fluxes. Another interesting approach is proposed in [10] where the elastic potential is modified to obey Von-Mises yield criterion.

In this study the motivation for developing an exact solution to the Riemann problem in non-linear elasticity is not for use within a numerical scheme, but rather as a tool for validating approximate techniques. In general, exact solutions of Riemann problems are iterative processes and their use in a numerical scheme would constitute an expensive overhead. Instead one can find approximate solutions, or solve exactly an approximation of the governing theory. Indeed in those studies mentioned above the numerical schemes employ approximate Riemann solvers. Titarev et al. [24] recently studied several approximate solvers for non-linear elasticity. It was shown that, except in some special circumstances, such approximate methods are sufficient to obtain high accuracy solutions.

Few authors have considered exact solutions of the Riemann problem in non-linear elasticity. In all but one of these studies solutions are obtained only for the special case of uniaxial deformations. Garaizar [6] presents a theoretical evaluation of the equations of elasticity and proposes an algorithm for uniaxial deformations; however, no numerical results are given. Titarev et al. [24] also solve the Riemann exactly for uniaxial deformations. Miller [15] proposed an exact iterative method for the solution of the Riemann problem of arbitrary hyperbolic systems of conservation laws, using the equations of non-linear elasticity as an example. Here, they appear to be the first to consider exact solutions for three-dimensional deformations. Their results highlighted large discrepancies between exact and approximated solutions of initial value problems and stands as an example of the need for exact solutions.

The purpose of the present work is to apply certain well established high–order shock capturing methods to the augmented one-dimensional equations of non-linear elasticity. The model of Godunov and Romenski [8] is considered and a characteristic tracing based approximate Riemann solver is extended to consider three-dimensional deformations, based upon the work in [24]. In comparison to the one-dimensional system for two-dimensional deformations, this requires the evaluation of an additional six equations, and an examination of the eigensystem reveals a total of seven characteristic fields. Similar wave profiles are found in magnetohydrodynamics (MHD) and in [1] it is shown that improved wave resolution can be achieved via high–order monotonicity preserving weighted essentially non-oscillatory (MPWENO) reconstruction. In particular these have benefits for for such problems where slow shocks proceed a faster moving wave, where the former can otherwise be insufficiently resolved. In order to assess these methods for non-linear elasticity exact solutions are desirable.

The proposed exact solution method requires systematic evaluation of the solutions across each characteristic wave. It is assumed that the Riemann problem solution comprises a central linearly degenerate contact wave, with all other waves being genuinly non-linear. In [15], where a similar approach is adopted, it is reported that these assumptions limit the applicability of the algorithm as a result of certain conditions, such as lack of genuine non-linearity, that can occur for non-linear elastic materials. Analysis of these conditions is not repeated here, but a discussion of the impact on the range of applicability of the scheme proposed in this paper is given in Section 3.6. Concisely, as a result of these conditions the present proposed exact solution proceedure is valid only for cases where all seven waves are distinct.

The rest of the paper proceeds as follows. In Section 2 the governing equations are presented along with an analysis of the characteristic decomposition. In Section 3 details are given of an exact iterative solution to the Riemann problem, while Section 4 outlines a numerical scheme. A comparative analysis between exact and numerical methods using example testcases is presented in Section 5 and finally conclusions are drawn in Section 6.

2. Governing theory

To describe processes in condensed media in the Eulerian reference frame the model of Godunov and Romenski [7] (and more recently [8]) is used. Here, the state of a solid is characterised by the elastic deformation gradient $F_{ij} = \partial x_i / \partial x_{0_j}$ (where x_i and x_{0_j} denote the fixed spatial coordinates and material coordinates of the unstressed reference state respectively), velocity u_i, and entropy S. The complete three dimensional system forms a hyperbolic system of conservation laws for momentum, strain, and energy. In Cartesian coordinates

$$\frac{\partial \rho u_i}{\partial t} + \frac{\partial \left(\rho u_i u_k - \sigma_{ik}\right)}{\partial x_k} = 0 \tag{1a}$$

$$\frac{\partial \rho F_{ij}}{\partial t} + \frac{\partial \left(\rho F_{ij} u_k - \rho F_{kj} u_i\right)}{\partial x_k} = 0 \tag{1b}$$

$$\frac{\partial \rho E}{\partial t} + \frac{\partial \left(\rho u_k E - u_i \sigma_{ik}\right)}{\partial x_k} = 0 \tag{1c}$$

Here, ρ is the density, σ the stress, $E = \left(\mathscr{E} + |u|^2/2\right)$ the total energy, with $\mathscr{E}$ the specific internal energy. Repeated indices denote summation (see Appendix). The system is closed by analytic formulae for the specific internal energy in terms of the parameters of state

$$\mathscr{E} = \mathscr{E}(F_{11},\, F_{12},\, \ldots,\, F_{33},\, S). \tag{2}$$

Density, temperature and the stress tensor are given by

$$\rho = \rho_0 / \det|F|, \tag{3}$$

$$T = \frac{\partial \mathscr{E}}{\partial S}, \tag{4}$$

$$\sigma_{ij} = \rho F_{ik} \frac{\partial \mathscr{E}}{\partial F_{jk}} \tag{5}$$

where ρ_0 denotes the density of the initial unstressed medium.

Using (14) it is possible to show that the combination of equations governing the conservation of strain conserve mass, by means of recovering the continuity equation

$$\frac{\partial \rho}{\partial t} + \frac{\partial \rho u_\alpha}{\partial x_\alpha} = 0. \tag{6}$$

Further this equation can be used in the development of numerical methods in place of one equation for deformation gradient in order to provide conservation of mass (see [24]).

It is remarked that using the form of the potential (2) does not guarantee that the stress tensor, Eq. (5), is symmetric. It is first necessary to discus the frame indifference of the internal energy density. This point is discussed in detail in [16] where it is shown that in order to satisfy frame indifference the internal energy must instead be expressed in terms of some symmetric strain tensor. Using for example the Finger tensor $G = F^{-T} F^{-1}$, then one might instead have

$$\mathscr{E} = \mathscr{E}(G_{11},\, G_{12},\, \ldots,\, G_{33},\, S). \tag{7}$$

It is shown in [8] that in terms of the Finger strain tensor the Murnaghan formula, Eq. (5), becomes

$$\sigma_{ij} = -2\rho G_{ik} \frac{\partial \mathscr{E}}{\partial G_{kj}}. \tag{8}$$

In [8] it is also pointed out that the symmetry of Eq. (8), using (7) still remains unclear, but that this can easily be established on the grounds that the internal energy density for a hyperelastic isotropic medium is

not an arbitrary function of G but rather depends on the invariants $I_1 = \mathrm{tr}(G)$, $I_2 = \frac{1}{2}\left[(\mathrm{tr}(G))^2 - \mathrm{tr}(G^2)\right]$, $I_3 = \det|G|$.

The equations for deformation gradient satisfy three compatibility constraints

$$\frac{\partial \rho F_{kj}}{\partial x_k} = 0, \ j = 1, 2, 3, \tag{9}$$

which hold for any time $t > 0$ if true for the initial data at $t = 0$. In fact, these constraints are a consequence of six compatibility conditions for the Lagrangian deformation gradient $f = F^{-1}$ which are derived as follows. First, consider the evolution equations for f_{ij} (see [8])

$$\frac{\partial f_{ij}}{\partial t} + u_k \frac{\partial f_{ij}}{\partial x_k} + f_{ik} \frac{\partial u_k}{\partial x_j} = 0.$$

By introducing the tensor $B_{ij} = f_{ik} b_{kj} / \det F$, where

$$b_{1i} = \frac{\partial f_{i3}}{\partial x_2} - \frac{\partial f_{i2}}{\partial x_3}, \ b_{2i} = \frac{\partial f_{i1}}{\partial x_3} - \frac{\partial f_{i3}}{\partial x_1}, \ b_{3i} = \frac{\partial f_{i2}}{\partial x_1} - \frac{\partial f_{i1}}{\partial x_2},$$

one can obtain as a consequence of the above equation for f_{ij}

$$\frac{\partial B_{ij}}{\partial t} + u_k \frac{\partial B_{ij}}{\partial x_k} = 0. \tag{10}$$

From these results it follows that if $B_{ij} = 0$ for the initial data, then it holds for any time. Therefore, because $b_{ij} = F_{ik} B_{kj} \det|F|$ and the tensor F_{ik} is positive defined, the same conclusion can be drawn for b_{kj}. Thus, six compatibility conditions for Lagrangian elastic deformations are obtained:

$$\frac{\partial f_{mn}}{\partial x_l} - \frac{\partial f_{ml}}{\partial x_n} = 0 \tag{11}$$

If these compatibility conditions hold for initial data, then they hold for any time. Finally, the following relation can be obtained

$$\frac{\partial \rho F_{kj}}{\partial x_k} = \rho F_{ij} F_{nm} \left(\frac{\partial f_{mn}}{\partial x_i} - \frac{\partial f_{mi}}{\partial x_n} \right), \ j = 1, 2, 3, \tag{12}$$

from which it can be concluded that the three constraints (9) are a consequence of six compatibility constraints (12).

The compatibility constraints (9) play an integral part in the necessary characteristic analysis. It is reported in [26] that for a similar Eulerian formulation of equations for non-linear elastic materials, a characteristic analysis of the quasi-linear system deduced directly by differentiation of the conservative equations produces characteristic speeds which are unphysical and leads to spurious eigenvector deficiency. The conservation laws used in [26] are based upon the inverse of the deformation gradient, f_{ij}, rather than the present formulation in terms of F_{ij}. Direct reduction of the conservative system (1) too leads to unphysical wave families. To overcome this, certain derivatives in the quasi-linear equations for F_{ij} obtained from Eq. (1b) can be replaced using the constraints (9). An alternative approach which elucidates the necessary use of the constraints and arrives at the same result is to replace Eq. (1b) with the following modified form derived in [19]

$$\frac{\partial \rho F_{ij}}{\partial t} + \frac{\partial \left(\rho F_{ij} u_k - \rho F_{kj} u_i \right)}{\partial x_k} = -u_i \beta_j, \tag{13}$$

where $\beta_j = \partial \rho F_{kj} / \partial x_k$. If deformations are elastic then $\beta_j = 0$ for all time if true for the initial conditions, and Eqs. (1b) and (13) are equivalent. Direct reduction of Eq. (13) to quasi-linear form gives the following equations for F_{ij}

$$\frac{\partial F_{ij}}{\partial t} + u_k \frac{\partial F_{ij}}{\partial x_k} - F_{kj} \frac{\partial u_i}{\partial x_k} = 0. \tag{14}$$

which leads to physically correct wavespeeds and a complete set of independent eigenvectors. Thus, equations for the deformation gradient can be considered in two different equivalent forms: conservative and non-conservative. The conservative form is used below for studying discontinuous solutions (shock and contact waves). As a result of the consequences discussed above the non-conservative form, Eq. (14), is used to obtain eigenfunctions required for the construction of rarefaction waves.

It is remarked that similar modified form of the governing system, Eq. (13), is performed in [13] for the equations in terms of f_{ij}. Not only is this done for the purpose of obtaining physically correct wavespeeds for the quasi-linear system, but also with the aim of improving the numerical algorithm. It is indicated that by performing a numerical discretization of (1) one can expect not to be finding a solution U but instead some modification of it, say U^{mod}, as a result of truncation errors. In turn it cannot be guaranteed that U^{mod} satisfies the compatibility constraints, which by definition if equal to zero in the initial conditions should remain equal at all other times. Further it is pointed out that the subsequent effects of errors remain unresolved in their entirety for equations of this form. It is suggested in [13] that Eq. (13) should instead be solved, i.e. a single set of transport equations, leaving only the question of whether the solution complies with the original system (1), (9). Whilst these complications do not arise in the one-dimensional system studied in this paper, since $\partial(\rho F_{1j})/\partial t = 0$, the methods are developed in the prospect of later application to multi-dimensional problems, in which case it is likely that these modifications are necessary.

The ensuing numerical methods are derived on the basis of the augmented one-dimensional system (taking $k = 1$ in Eqs. (1a),(1c),(13)), which can be written in matrix form as

$$\frac{\partial U}{\partial t} + \frac{\partial \mathscr{F}}{\partial x} = -S^c. \tag{15}$$

with

$$U = \begin{pmatrix} \rho u \\ \rho F^T e_1 \\ \rho F^T e_2 \\ \rho F^T e_3 \\ \rho E \end{pmatrix}, \ \mathscr{F} = \begin{pmatrix} u_1 \rho u - \sigma e_1 \\ 0 \\ u_1 \rho F^T e_2 - u_2 \rho F^T e_1 \\ u_1 \rho F^T e_3 - u_3 \rho F^T e_1 \\ u_1 \rho E - (\sigma u) e_1 \end{pmatrix}, \ S^c = \begin{pmatrix} 0 \\ 0 \\ u_2 \frac{\partial}{\partial x} \rho F^T e_1 \\ u_3 \frac{\partial}{\partial x} \rho F^T e_1 \\ 0 \end{pmatrix},$$

where e_k are the Cartesian unit vectors and M^T denotes the transpose of the vector or tensor M. By introducing the vector of primitive variables $W = \big(u,\ F^T e_1,\ F^T e_2,\ F^T e_3,\ S\big)$, Eq. (15) can be rewritten as a quasi-linear system

$$\frac{\partial W}{\partial t} + \mathscr{A} \frac{\partial W}{\partial x} = 0, \tag{16}$$

with the Jacobian

$$\mathscr{A} = \begin{pmatrix} u_1 I & -A^{11} & -A^{12} & -A^{13} & -B^1 \\ -F^T E_{11} & u_1 I & 0 & 0 & 0 \\ -F^T E_{12} & 0 & u_1 I & 0 & 0 \\ -F^T E_{13} & 0 & 0 & u_1 I & 0 \\ 0 & 0 & 0 & 0 & u_1 \end{pmatrix}. \tag{17}$$

Here, E_{ij} represents the unit dyads $E_{ij} = e_i \otimes e_j^T$, I is the identity matrix, and the following coefficients are defined

$$A_{ij}^{1\beta} = \frac{1}{\rho} \frac{\partial \sigma_{1i}}{\partial F_{\beta j}}, \qquad B_i^1 = \frac{1}{\rho} \frac{\partial \sigma_{1i}}{\partial S}. \tag{18}$$

If λ denotes the wavespeeds then the characteristic polynomial for (17) ($|\mathscr{A} - \lambda I| = 0$) has the form

$$(u - \lambda)^7 \det \left| \Omega - (u - \lambda)^2 I \right| = 0,$$

where Ω is the *acoustic tensor*

$$\Omega_{ij} = A_{ik}^{1j} F_{1k}. \tag{19}$$

Due to the hyperbolicity of the system (15), the tensor Ω is positive definite and thus by defining the diagonal matrix of positive eigenvalues $D = \mathrm{diag}\left(\sqrt{\lambda_{ac_1}},\ \sqrt{\lambda_{ac_2}},\ \sqrt{\lambda_{ac_3}}\right)$, with $\lambda_{ac_3} \leq \lambda_{ac_2} \leq \lambda_{ac_1}$, and the orthogonal matrix Q, (19) can be rewritten

$$\Omega = Q^{-1} D^2 Q. \tag{20}$$

The diagonal matrix of eigenvalues is thus given by (assuming the order $u_1 - \sqrt{\lambda_{ac_1}} \leq u_1 - \sqrt{\lambda_{ac_2}} \leq \ldots \leq u_1 \leq \ldots \leq u_1 I + \sqrt{\lambda_{ac_1}}$)

$$\Lambda = \mathrm{diag}\left(u_1 I - D,\ u_1 I,\ u_1 I,\ u_1,\ u_1 I + \pi D \pi\right), \tag{21}$$

where the permutation matrix π is defined as

$$\pi = \begin{pmatrix} 0 & 0 & 1 \\ 0 & 1 & 0 \\ 1 & 0 & 0 \end{pmatrix},$$

with the matrix of left eigenvectors

$$L = \begin{pmatrix} DQ & QA^{11} & QA^{12} & QA^{13} & QB^1 \\ 0 & \frac{1}{F_{11}}(F_{12}E_{11} + F_{13}E_{21}) - E_{12} - E_{23} & \frac{1}{F_{11}}(F_{12}E_{31}) - E_{32} & 0 & 0 \\ 0 & 0 & \frac{1}{F_{11}}(F_{13}E_{11}) - E_{13} & \frac{1}{F_{11}}(F_{12}E_{21} + F_{13}E_{31}) - E_{22} - E_{33} & 0 \\ 0 & 0 & 0 & 0 & 1 \\ \pi DQ & -\pi QA^{11} & -\pi QA^{12} & -\pi QA^{13} & -\pi QB^1 \end{pmatrix}. \tag{22}$$

Using the assumption that the right eigenvectors are orthonormal to the left ($RL = I$)

$$R = \begin{pmatrix} \frac{1}{2}Q^{-1}D^{-1} & 0 & 0 & \frac{1}{2}Q^{-1}D^{-1}\pi \\ \frac{1}{2}\left(F^T e_1\right) \otimes \left(e_1^T Q^{-1} D^{-2}\right) & \left(F^T e_1\right) \otimes \left(e_1^T T_1\right) - E_{21} - E_{32} & \left(e_1^T \Omega^{-1} B^1\right) F^T e_1 & -\frac{1}{2}\left(\left(F^T e_1\right) \otimes \left(e_1^T Q^{-1} D^{-2}\right)\right)\pi \\ \frac{1}{2}\left(F^T e_1\right) \otimes \left(e_2^T Q^{-1} D^{-2}\right) & \left(F^T e_1\right) \otimes \left(e_2^T T_1\right) - E_{23} & \left(e_2^T \Omega^{-1} B^1\right) F^T e_1 & -\frac{1}{2}\left(\left(F^T e_1\right) \otimes \left(e_2^T Q^{-1} D^{-2}\right)\right)\pi \\ \frac{1}{2}\left(F^T e_1\right) \otimes \left(e_3^T Q^{-1} D^{-2}\right) & \left(F^T e_1\right) \otimes \left(e_3^T T_1\right) & \left(e_3^T \Omega^{-1} B^1\right) F^T e_1 & -\frac{1}{2}\left(\left(F^T e_1\right) \otimes \left(e_3^T Q^{-1} D^{-2}\right)\right)\pi \\ 0 & 0 & 1 & 0 \\ 0 & 0 & 0 & 0 \\ \left(F^T e_1\right) \otimes \left(e_1^T T_2\right) & \left(e_1^T \Omega^{-1} B^1\right) F^T e_1 & -\frac{1}{2}\left(\left(F^T e_1\right) \otimes \left(e_1^T Q^{-1} D^{-2}\right)\right)\pi & \\ \left(F^T e_1\right) \otimes \left(e_2^T T_2\right) - E_{31} & \left(e_2^T \Omega^{-1} B^1\right) F^T e_1 & -\frac{1}{2}\left(\left(F^T e_1\right) \otimes \left(e_2^T Q^{-1} D^{-2}\right)\right)\pi & \\ \left(F^T e_1\right) \otimes \left(e_3^T T_2\right) - E_{22} - E_{33} & \left(e_3^T \Omega^{-1} B^1\right) F^T e_1 & -\frac{1}{2}\left(\left(F^T e_1\right) \otimes \left(e_3^T Q^{-1} D^{-2}\right)\right)\pi & \\ 0 & 1 & 0 & \end{pmatrix}, \tag{23}$$

with

$$T_1 = \Omega^{-1}\left(A^{11}E_{21} + A^{11}E_{32} + A^{12}E_{23}\right),$$
$$T_2 = \Omega^{-1}\left(A^{12}E_{31} + A^{13}E_{22} + A^{13}E_{33}\right).$$

Using these results it is seen that there are seven linear degenerate ($r_i \cdot \nabla_w \lambda_i = 0$, where r_i denotes the i-th column vector of R) waves with equal velocity u_1, and six genuinly non-linear ($r_i \cdot \nabla_w \lambda_i \neq 0$) waves with velocities $u_1 I - D$ and $u_1 I + D$.

Here, the eigenvectors have been written in compact form. Since they play a fundamental role in solving the Riemann problem both exactly and approximately, and to improve reproducibility, the expanded matrices are presented in the Appendix. Evaluating the acoustic tensor, (19), analytically is relatively straightforward but cumbersome, requiring evaluation of a large number of derivatives to formulate the coefficients (18). Computation of the diagonal matrix D and orthogonal matrix Q is performed numerically using those methods in [22].

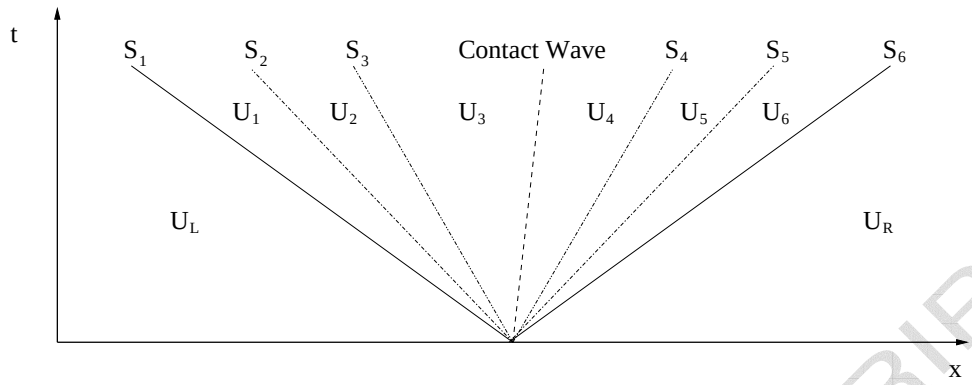

Figure 1: Illustration of the Riemann problem for non-linear elasticity in space-time. The wavespeeds for the six genuinely non-linear waves are denoted by S_j, $1 \leq j \leq 6$. Between each wave the state is constant denoted by U_j, $1 \leq j \leq 6$. The states U_L and U_R correspond to the initial left and right conditions respectively.

3. Exact Riemann problem solution

In this section an exact iterative method is derived for the solution of the Riemann problem: solutions of the system (15) subject to the initial conditions

$$U(x, t=0) = \begin{cases} U_L & \text{if} \quad x \leq x_0 \\ U_R & \text{if} \quad x > x_0 \end{cases}, \tag{24}$$

where x_0 is the position of the discontinuity in the initial data. Depending on how the initial states in (24) are chosen the solution of the Riemann problem for non-linear elasticity can consist of up to eight constant states separated by seven distinct waves. These are from left to right: a longitudinal wave, two tranverse shear waves, a contact wave, two more shear waves and a further longitudinal wave (Figure 3).

Considering all waves to be distinct, then the solution across each is uniquely determine once one state either side and the wavespeed are known. To elaborate, given an estimate of the states on the left and right in the initial data, (24), and also for the intermediate six constant states U_j, $1 \leq j \leq 6$, then the the type of wave present can be determined by analysing for each the inclination of characteristics

$$\begin{cases} |\lambda^+| < |\lambda^-| & \Longrightarrow \quad \text{shock wave} \\ |\lambda^+| > |\lambda^-| & \Longrightarrow \quad \text{rarefaction wave} \end{cases} \tag{25}$$

Here λ is the respective characteristic speed, whilst $\pm$ indicates the state from which this is analysed: for any quantity ϕ, ϕ^+ denotes evaluation from the upstream state and ϕ^- denotes evaluation from the downstream state. This notation shall be adopted throughout. The wavespeeds, S_j, $1 \leq j \leq 6$, are determined differently for either shocks or refractions.

On this basis then, given the wave types and speeds the inner most states either side of the contact wave (U_3 and U_4 in Figure 3) can be computed. Treating the collective waves to the left and to the right of the contact independently, the solution across the three waves to the left are first evaluated, and then likewise for those to the right. The found states must satisfy by definition certain continuity conditions across the contact. Any residual error then is reflective of errors in the estimates of the wavespeeds. For each iteration the residual errors can be used to obtain improved estimates of the wavespeeds until some convergence criteria is satisfied.

It is intuitive to now consider solutions for each of the non-linear waves will, before summarising the implementation.

3.1. Contact waves

Consider a discontinuity propagating with velocity $\mathscr{D}$. For the system (15) the Rankine-Hugoniot relations connecting the left and right states are given by

$$[U]\,\mathscr{D} = [\mathscr{F}]\,, \tag{26}$$

where for any quantity ϕ, $[\phi] = \phi^- - \phi^+$. An isolated contact discontinuity is defined by the condition that the normal velocity component does not change across it

$$u_1^+ = u_1^- = \mathscr{D}.$$

From (15) and taking into account the compatibility conditions (9), the following equalities are obtained

$$[u] = \left[\rho F^T e_1\right] = [\sigma_{11} e_1] = 0. \tag{27}$$

The inner most states either side of the contact wave, U_3 and U_4, are uniquely determined by the initial left and right states in (24), and estimates of the wavespeeds S_j, $1 \leq j \leq 6$. In turn these inner states should satisfy those continuity conditions (27). Therefore using (27) six non-linear equations can be written for the six unknown wavespeeds

$$\mathscr{R}_c(S_1, S_2, \ldots, S_6) = \begin{pmatrix} u^+(U_3) - u^-(U_4) \\ \sigma^+(U_3)e_1 - \sigma^-(U_4)e_1 \end{pmatrix} = 0. \tag{28}$$

In general Eq. (28) will not be satisfied by the initial guess, and instead it is expected that $|\mathscr{R}_c| > 0$. Therefore (28) can be solved for improved estimates of the wavespeeds using Newton's method

$$S^n = S^{n-1} - \left(\partial \mathscr{R}_c / \partial S\right)^{-1} \mathscr{R}_c. \tag{29}$$

The six-by-six Jacobian in (29) can be evaluated using perturbations of each wavespeed. A second order approximation can be written

$$\frac{\partial \mathscr{R}_{c_i}}{\partial S_j} \approx \frac{\mathscr{R}_{c_i}(S_j + \varepsilon) - \mathscr{R}_{c_i}(S_j - \varepsilon)}{2\varepsilon} \tag{30}$$

Experience shows that choosing $\varepsilon = 1 \cdot 10^{-6}$ is sufficient to obtain converged solutions.

3.2. Shock waves

Consider a shock wave propagating with a velocity $\mathscr{S}$. Based upon the Rankine-Hugoniot relations (26) then

$$\mathscr{R}_s = \mathscr{F}(U^+) - \mathscr{F}(U^-) - \mathscr{S}\left(U^+ - U^-\right) = 0. \tag{31}$$

Following the method of solving for the upstream state U^+ from the known downstream state U^- and shock speed $\mathscr{S}$, it is deduced that (31) is a set of non-linear relations in terms of U^+. Using Newton's method then

$$U^{-,n} = U^{-,n-1} - \left(\partial \mathscr{R}_s / \partial U^-\right)^{-1} \mathscr{R}_s. \tag{32}$$

If (32) is being solved from the left then $\mathscr{S} = S_j$, $U^+ = U_{j-1}$ with $U_0 = U_L$, giving $U_j = U^-$, $1 \leq j \leq 3$. Similarly for the right $\mathscr{S} = S_j$, $U^+ = U_{j+1}$ with $U_7 = U_R$, giving $U_j = U^-$, $4 \leq j \leq 6$.

3.3. Rarefaction waves

For rarefaction waves the theory presented in [12] is followed. If r_j denotes the j-th column vector in (23) then across a rarefaction wave

$$\frac{\partial W}{\partial \xi} = \frac{r_j(W)}{r_j(W) \cdot \nabla_w \lambda_j(W)}, \tag{33}$$

where $\lambda_j(W^-) \leq \xi = x/t \leq \lambda_j(W^+)$ and ∇_w denotes the gradient operator with respect to components of the vector of primitive variables, W.

An important consideration when solving (33) is that the solution is parameterised by the characteristic evaluated from the upstream state, $\lambda(W^-)$, and solving (33) otherwise would lead to a multi-valued function [12]. In the solution of the Riemann problem it is assumed that for each genuinely non-linear wave the corresponding downstream state is known. Solving across rarefaction waves becomes therefore an iterative process. It is convenient to consider this solution for each side of the contact wave: for waves on the left solve

$$\mathscr{R}_r = W_{j-1} - W^+(W_j) = 0, \tag{34}$$

and likewise for the right

$$\mathscr{R}_r = W_{j+1} - W^+(W_j) = 0, \tag{35}$$

where in each case $W^+(W_j)$ denotes solution of (33) using an estimate of the upstream state $W^- = W_j$. Similar to (32) for shock waves, Eq. (34) and Eq. (35) can be solved using Newton's method

$$W^{-,n} = W^{-,n-1} - \left(\partial \mathscr{R}_r / \partial W^-\right)^{-1} \mathscr{R}_r. \tag{36}$$

As an initial guess the last known solution of W_j can be taken.

Eq. (33) can be integrated using the classical fourth-order Runge–Kutta method. It is necessary in some cases to subdivide the integral into n parts; experience shows for those testcases here $n = 10$ is sufficient. The step size can be taken as $\Delta\xi_j = \lambda_j(W_{j-1}) - S_j$, $1 \le j \le 3$, for the left and $\Delta\xi_j = \lambda_{j+7}(W_{j+1}) - S_j$, $4 \le j \le 6$, for the right. An additional complexity of solving across rarefaction waves is the evaluation of the right-hand-side of (33). Taking as an example the wave $\lambda = u_1 - \sqrt{\lambda_{ac_k}}$, expanding the denominator in (33) gives

$$r_k \cdot \nabla_w (u_1 - D_{kk}) = \left(Q^{-1} D^{-1}\right)_{1k} - \sum_{j,m=1}^{3} F_{1j} \left(Q^{-1} D^{-2}\right)_{mk} \frac{\partial D_{kk}}{\partial F_{mj}}. \tag{37}$$

When computing the diagonalisation of the acoustic tensor, Eq. (20), it is more convenient to do so numerically rather than derive lengthy expressions for the corresponding third order polynomial. This omission of closed form solutions for the acoustic wavespeeds means some other approach is required if the derivatives with respect to deformation in Eq. (37) are to be evaluated analytically. The method in [15] provides a convenient way to find analytic solutions for each of these terms. Considering the diagonalisation of the acoustic tensor, Eq. (20), the following equalities are obtained

$$\nabla_F \left(\Omega Q^{-1}\right) = \nabla_F \left(Q^{-1} D^2\right),$$

$$\nabla_F (\Omega) Q^{-1} + \Lambda \nabla_F \left(Q^{-1}\right) = \nabla_F \left(Q^{-1}\right) D^2 + Q^{-1} \nabla_F \left(D^2\right),$$

$$Q \nabla_F (\Omega) Q^{-1} + D^2 Q \nabla_F \left(Q^{-1}\right) = Q \nabla_F \left(Q^{-1}\right) D^2 + I \nabla_F \left(D^2\right),$$

where ∇_F denotes the gradient operator with respect to deformation. Taking only the diagonal components

$$\nabla_F \left(D_{kk}^2\right) = Q_{km} \nabla_F \left(\Omega_{mj}\right) Q_{jk}^{-1}. \tag{38}$$

Evaluating derivatives of the acoustic tensor, although rather lengthy, is relatively straightforward.

3.4. Solution proceedure

Here, the implementation is summarised

Step 1: *Initialise solution.* Given an initial estimate of the piecewise constant states U_j, $1 \le j \le 6$, between each of the non-linear waves, and the initial left and right states U_L, U_R in (24), one determines the wave types by assessing the inclination of characteristics (25). Once the wave types are known proceed to evaluate an initial estimate of the wave speeds S_j, $1 \le j \le 6$ using $S_j = \mathscr{S}$ from (31) for a shock, and $S_j = \lambda_j$, $1 \le j \le 3$, or $S_j = \lambda_{j+7}$, $4 \le j \le 6$, from (21) for left and right waves respectively in the case of a rarefaction.

Step 2: *Compute residual errors*. Given an estimate of the wavespeeds S_j, $1 \leq j \leq 6$ and the left and right states U_L, U_R, and knowing the wave types, systematically find the solution U^- across each wave (in each case the corresponding downstream state U^+ is known). Starting with the left hand state U_L move upstream solving across each wave for $U_j = U^-$, $1 \leq j \leq 3$, taking $U^+ = U_{j-1}$, with $U_0 = U_L$. Continue this procedure until a solution is found for the state immediately left of the contact wave U_3. Likewise evaluate upstream starting from the right initial state U_R, where for each wave take $U^+ = U_{j+1}$, $1 \leq j \leq 3$, with $U_7 = U_R$, until a solution is found for the state immediately to the right of the contact wave U_4. Thus evaluate the truncation errors, (28), in continuity across the contact wave.

Step 3 *Estimate new wavespeeds*. If from *Step 2* $\sum_{i=1}^{6} |\mathscr{R}_{c_i}| > \epsilon$, where ϵ is the desired tolerance, then use (29) to improve the estimates of the wavespeeds. Evaluate the Jacobian in (29) using small perturbations of each wavespeed and re-evaluating in each case *Step 2*. With the new wavespeeds again re-evaluate *Step 2* until $\sum_{i=1}^{6} |\mathscr{R}_{c_i}| < \epsilon$ is satisfied.

Experience shows that with a good initial guess the solution will converge in three to four iterations to a tolerance of $\sum_{i=1}^{6} |\mathscr{R}_{c_i}| < 10^{-8}$.

3.5. Provision of the initial guess

The final detail of the exact solution method is the specification of initial estimates of the states U_i, $1 \leq i \leq 6$. One choice would be to use the linearised solver proposed in the next section. In most cases a linearised solution is sufficient, but in some special cases will fail (see [24]). In such circumstances one could instead interpolate a solution from the results of any scheme such as Lax-Friedrich, which approximates directly the governing model rather than solves exactly an approximation of it, run on a sufficiently fine grid. Such a method has no knowledge of the characteristic structure and although diffusive (hence the need for fine meshes, especially where amplitudes of waves or the difference in speeds of adjacent waves is small) one can be assured that the solution is a faithful representation of the exact solution. The method of solving the Riemann problem exactly hinges on this ability to obtain a good initial guess of the states either side of each of the waves in order to determine the wavetypes.

3.6. Limitations of the exact solver

The proposed method of obtaining exact solutions to Riemann problems in non-linear elasticity is limited to those cases where all waves are distinct as a result of the following assumptions that are made: all waves are genuinly non-linear except for the central contact wave which is linearly degenerate; the wave type is determinable by analysing the inclination of characteristics. In [15] conditions are discussed where these assumptions would cause the method to fail to reach an exact solution. For example it is reported that for the case where transverse wavespeeds coincide, which for an isotropic hyperelastic material occurs when the internal energy density resides on the reference hydrostat, there is a lack of genuine non-linearity. Modifications are proposed in [15] that overcome these difficulties and restore the generality of the scheme. These modifications have not been implemented in the present study, hence the limitation to cases where all waves are distinct. The sought solutions cannot therefore be considered general, but do provide adequate tests for examining certain capabilites of the proposed numerical algorithms discussed next.

4. Numerical scheme

The system (15) is solved numerically using a finite volume discretisation with cell averaged data stored at the cell centres, denoted by the indices i. Discretisation of the time derivatives is achieved by re-expressing (15) as

$$\frac{\mathrm{d}}{\mathrm{d}t} U_i(t) = L_i(U), \tag{39}$$

with

$$L_i(U) = -\frac{\mathscr{F}\left(U(x_{i+1/2},t)\right) - \mathscr{F}\left(U(x_{i-1/2},t)\right)}{\Delta x}, \tag{40}$$

where $i+1/2$ denotes cell boundaries and $U_i(t)$ is the space average of the solution in the i-th cell at time t

$$U_i(t) = \frac{1}{\Delta x}\int_{x_{i-1/2}}^{x_{i+1/2}} U(x,t)\mathrm{d}x.$$

Eq. (39) is integrated using the third-order TVD Runge–Kutta scheme

$$\begin{aligned} U_i^{(1)} &= U_i^n + \Delta t L_i(U^n) \\ U_i^{(2)} &= U_i^n + \frac{\Delta t}{4}\left[L_i(U^n) + L_i(U^{(1)})\right] \\ U_i^{n+1} &= U_i^n + \frac{\Delta t}{6}\left[L_i(U^n) + L_i(U^{(1)}) + 4L_i(U^{(2)})\right] \end{aligned}, \tag{41}$$

where n denotes the current iteration. The global timestep is found from

$$\Delta t = \mathrm{CFL}\frac{\Delta x}{\max\left(|u_1| + \sqrt{\lambda_{ac_1}}\right)},$$

where $0 \leq \mathrm{CFL} \leq 1$ is an adjustable scaler parameter used to control the timestep so as to satisfy the Courant-Friedrichs-Lewy condition.

In the numerical method the convective flux terms in (40) are discretised using the well known method of Godunov. Therefore solution of a Riemann problem is required at the boundaries of each cell in the computational mesh. Exact solutions to these problems following the procedure outlined in the preceeding section, are somewhat complex and expensive. In general one can instead apply an approximate solution method, such as those described in [25, 4]. Titarev et al. [24] examined the performance of a number of different approximate Riemann solvers for the equations of non-linear elasticity. They found that a linearised solver based upon characteristic tracing yielded a good balance between accuracy and cost. It also has the advantage of recognising all waves in the solution and is shown to exceed the ability of some alternative upwind methods in resolving delicate features such as contact discontinuities. Although approximate Riemann solvers based upon linearising the governing equations have well known drawbacks, such as the production of entropy violating shock waves where there are sonic rarefactions, it is pointed out in [24] that these conditions are rare in solid media. For all intended purposes a characteristics based method can be expected to perform well.

4.1. Flux approximation

Consider the non-linear system (16). If it is assumed that the Jacobian $\mathscr{A}$ is evaluated at some constant state $\widehat{W}$ such that $\widehat{A} = A(\widehat{W})$ consists entirely of constant coefficients, then in turn the corresponding eigenvalues and eigenvectors are constant, $\widehat{\Lambda} = \Lambda(\widehat{W})$, $\widehat{L} = L(\widehat{W})$, $\widehat{R} = R(\widehat{W})$. If $\mathscr{Q} = \widehat{L}W$ is defined as the vector of characteristic variables, then (16) can be rewritten in the decoupled characteristic form

$$\left(\frac{\partial}{\partial t} + \widehat{\lambda}_j\frac{\partial}{\partial x}\right)\mathscr{Q}_j = 0, \qquad 1 \leq j \leq 13. \tag{42}$$

Since, from (42), $\mathscr{Q}_j$ is invariant along the characteristic of slope $\widehat{\lambda}_j$, the solution for any Cauchy problem is simply $\mathscr{Q}_j(x,t) = \mathscr{Q}_j\left(W(x-\widehat{\lambda}_j t)\right)$, which gives

$$W(x,t) = \widehat{R}\mathscr{Q}(x,t). \tag{43}$$

In order to maintain high order accuracy it is necessary to reexpress the invariants in terms of conserved variables. The extension is based upon the ideas in [5, 2] for the compressible Euler equations. The resultant

Riemann solver has also been successfully applied to incompressible fluid dynamics [4, 3]. The derivation here follows the tensorial approach presented in [20]. From (42) the invariants $\partial\mathscr{Q} = \widehat{L}\cdot\partial W$ can be transformed simply as $\partial\mathscr{Q} = \widehat{L}\widehat{C}\cdot\partial U$, where $\widehat{C} \equiv (\partial\widehat{W}/\partial\widehat{U})$. Partial derivatives of the velocity vector and deformation tensor can be expressed in terms of partial derivatives of conserved variables according to

$$\partial u = \frac{1}{\rho}(\partial(\rho u) - u\partial\rho), \tag{44}$$

$$\partial F = \frac{1}{\rho}(\partial(\rho F) - F\partial\rho), \tag{45}$$

For entropy (from (2) $S = S(\mathscr{E},\, F_{11},\, F_{12},\, \ldots,\, F_{33})$)

$$\partial S = \frac{\mathrm{d}S}{\mathrm{d}\mathscr{E}}\partial\mathscr{E} + \sum_{i,j=1}^{3}\frac{\mathrm{d}S}{\mathrm{d}F_{ij}}\partial F_{ij}. \tag{46}$$

Using the definition of total energy

$$\partial(\rho\mathscr{E}) = \partial(\rho E) - u_i\partial(\rho u)_i + \frac{1}{2}|u|^2\partial\rho,$$

in (46) gives

$$\partial S = \frac{1}{\rho}\left(\frac{\mathrm{d}S}{\mathrm{d}\mathscr{E}}(\partial(\rho E) - u_i\partial(\rho u)_i + \frac{1}{2}|u|^2\partial\rho - \mathscr{E}\partial\rho) + \sum_{i,j=1}^{3}\frac{\mathrm{d}S}{\mathrm{d}F_{ij}}(\partial(\rho F)_{ij} - F_{ij}\partial\rho)\right). \tag{47}$$

Since density is a function of $\det|\rho F|$, $\rho^2 = \det|\rho F|/\rho_0$

$$\partial\rho = \frac{1}{2}\sum_{i,j=1}^{3}F_{ij}^{-T}\partial F_{ij}. \tag{48}$$

Partial derivatives with respect to density then in (44), (45) and (47) can be replaced with (48). In matrix form

$$C = -\frac{1}{2\rho}\begin{pmatrix} -2I & u\otimes\left(e_1^TF^{-T}\right) & u\otimes\left(e_2^TF^{-T}\right) & u\otimes\left(e_3^TF^{-T}\right) & 0\\ 0 & \left(F^Te_1\right)\otimes\left(e_1^TF^{-T}\right) - 2I & \left(F^Te_1\right)\otimes\left(e_2^TF^{-T}\right) & \left(F^Te_1\right)\otimes\left(e_3^TF^{-T}\right) & 0\\ 0 & \left(F^Te_2\right)\otimes\left(e_1^TF^{-T}\right) & \left(F^Te_2\right)\otimes\left(e_2^TF^{-T}\right) - 2I & \left(F^Te_2\right)\otimes\left(e_3^TF^{-T}\right) & 0\\ 0 & \left(F^Te_3\right)\otimes\left(e_1^TF^{-T}\right) & \left(F^Te_3\right)\otimes\left(e_2^TF^{-T}\right) & \left(F^Te_3\right)\otimes\left(e_3^TF^{-T}\right) - 2I & 0\\ 2\dfrac{\mathrm{d}S}{\mathrm{d}\mathscr{E}}u^T & -2\dfrac{\mathrm{d}S}{\mathrm{d}e_1^TF} - e_1^TF^{-T}T_3 & -2\dfrac{\mathrm{d}S}{\mathrm{d}e_2^TF} - e_2^TF^{-T}T_3 & -2\dfrac{\mathrm{d}S}{\mathrm{d}e_3^TF} - e_3^TF^{-T}T_3 & -2\dfrac{\mathrm{d}S}{\mathrm{d}\mathscr{E}} \end{pmatrix}, \tag{49}$$

with

$$T_3 = \frac{\mathrm{d}S}{\mathrm{d}\mathscr{E}}(\frac{1}{2}|u|^2 - \mathscr{E}) - \sum_{i,j=1}^{3}\frac{\mathrm{d}S}{\mathrm{d}F_{ij}}F_{ij}.$$

The inverse of (49) is given by

$$C^{-1} \equiv \frac{\partial U}{\partial W} = -\rho \begin{pmatrix} -I & u \otimes \left(e_1^T F^{-T}\right) & u \otimes \left(e_2^T F^{-T}\right) \\ 0 & \left(F^T e_1\right) \otimes \left(e_1^T F^{-T}\right) - I & \left(F^T e_1\right) \otimes \left(e_2^T F^{-T}\right) \\ 0 & \left(F^T e_2\right) \otimes \left(e_1^T F^{-T}\right) & \left(F^T e_2\right) \otimes \left(e_2^T F^{-T}\right) - I \\ 0 & \left(F^T e_3\right) \otimes \left(e_1^T F^{-T}\right) & \left(F^T e_3\right) \otimes \left(e_2^T F^{-T}\right) \\ -u^T & \dfrac{\mathrm{d}\mathscr{E}}{\mathrm{d}e_1^T F} - e_1^T F^{-T}(\frac{1}{2}|u|^2 + \mathscr{E}) & \dfrac{\mathrm{d}\mathscr{E}}{\mathrm{d}e_2^T F} - e_2^T F^{-T}(\frac{1}{2}|u|^2 + \mathscr{E}) \end{pmatrix} \begin{pmatrix} u \otimes \left(e_3^T F^{-T}\right) & 0 \\ \left(F^T e_1\right) \otimes \left(e_3^T F^{-T}\right) & 0 \\ \left(F^T e_2\right) \otimes \left(e_3^T F^{-T}\right) & 0 \\ \left(F^T e_3\right) \otimes \left(e_3^T F^{-T}\right) - I & 0 \\ \dfrac{\mathrm{d}\mathscr{E}}{\mathrm{d}e_3^T F} - e_3^T F^{-T}(\frac{1}{2}|u|^2 + \mathscr{E}) & -\frac{\mathrm{d}\mathscr{E}}{\mathrm{d}S} \end{pmatrix}. \tag{50}$$

Thus the solution in terms of conserved variables becomes

$$U(x,t) = \widehat{C}^{-1}\widehat{R}\mathscr{Q}_c(x - \widehat{\lambda}t). \tag{51}$$

where $\mathscr{Q}_c = \widehat{L}\widehat{C} \cdot U$.

On a computational mesh these linearised problems are solved at each intercell boundary, $i+1/2$. Locally then one is solving exactly an approximation of the non-linear system (15). There is no set way in which the constant state $\widehat{W}_{i+1/2}$ should be chosen to evaluate the coefficients. Here, an arithmetic mean of the adjoining left and right cell centre states is used

$$\widehat{W}_{i+1/2} = \frac{1}{2}\left(W_i + W_{i+1}\right). \tag{52}$$

A convenient function that achieves the solution (51) is [5]

$$\mathscr{Q}(x_{i+1/2} - \widehat{\lambda}_{j;i+1/2}t) = \left(\frac{1}{2} + \psi_{j;i+1/2}\right)\mathscr{Q}^L_{i+1/2} + \left(\frac{1}{2} - \psi_{j;i+1/2}\right)\mathscr{Q}^R_{i+1/2}, \tag{53}$$

with

$$\psi_{j;i+1/2} = \frac{1}{2}\frac{\widehat{\lambda}_{j;i+1/2}}{|\widehat{\lambda}_{j;i+1/2}| + \varepsilon}, \qquad \widehat{\lambda}_{j;i+1/2} = \lambda_j(\widehat{W}_{i+1/2})$$

where $\mathscr{Q}^L_{i+1/2}$ and $\mathscr{Q}^R_{i+1/2}$ represent the left and right characteristic states adjacent to the boundary found by some high-order reconstruction method, and ε is a small number to prevent division by zero. Alternatively by choosing $\mathscr{Q}^L_{i+1/2} = \mathscr{Q}(U_i)$ and $\mathscr{Q}^R_{i+1/2} = \mathscr{Q}(U_{i+1})$ a first order upwind method is recovered.

The found solution (51) can then be used to construct the flux term in (40).

4.2. High-order spatial reconstruction

The outlined characteristic-based flux is used directly to construct high-order finite-volume schemes, in which the boundary-extrapolated values are obtained from cell averages by means of a high order polynomial reconstruction. In the present paper state-of-art weighted essentially non-oscillatory (WENO) schemes of third, fifth and ninth order of spatial accuracy are used. For a detailed description of the WENO reconstructions and schemes see [9, 1], as well as [14, 23] for applications to turbulence, and the references therein. Below, a brief description is provided of the most practical fifth-order reconstruction procedure.

For a scalar function $\phi(x)$ the fifth order accurate left boundary extrapolated value $\phi^L_{i+1/2}$ is defined in terms of cell averaged values ϕ_i as

$$\phi^L_{i+1/2} = \omega_0 v_0 + \omega_1 v_1 + \omega_2 v_2, \tag{54}$$

where v_k is the extrapolated value obtained from cell averages in the k^{th} stencil $S_k = (i-k, i-k+1, i-k+2)$ and ω_k, $k = 1, 2, 3$, are nonlinear WENO weights given by

$$\omega_k = \frac{\alpha_k}{\sum_{l=0}^{3} \alpha_l}, \quad \alpha_0 = \frac{3}{10(\beta_0 + \varepsilon)^2}, \quad \alpha_1 = \frac{3}{5(\beta_1 + \varepsilon)^2}, \quad \alpha_2 = \frac{1}{10(\beta_2 + \varepsilon)^2}.$$

Here, a small parameter ε is introduced to avoid division by zero, for which a recommended value and that used here is $\varepsilon = 10^{-6}$. The expressions for the extrapolated values v_k and smoothness indicators β_k can be found in [9] and are thus omitted. The right value $\phi^R_{i+1/2}$ is obtained by symmetry.

It was found that component-wise reconstruction leads to severe oscillations for those testcases considered here and, not surprisingly, are much worse than those observed for the Euler equations [18]. Thus, in practical calculations the outlined scalar reconstruction procedure is carried out in characteristic variables rather than conservative variables and (54) is applied to each characteristic field. It was also found that for the nonlinear elasticity equations the WENO reconstructions of fifth- and higher-orders may still produce oscillatory results around particularly steep gradients. To avoid spurious oscillations, the monotonicity preserving modification of [1] can be used, which is effectively a further limiting step applied to the WENO extrapolated values. In what follows the j-th order WENO scheme will be referred to as WENO-j and likewise for the monotonicity preserving WENO scheme MPWENO-j.

5. Examples

Testcases are now provided to compare the numerical schemes against exact solutions. Before proceeding, the closure relation (2) must be specified. The specific internal energy can be decomposed into potentials describing the hydrostatic and thermal energy density, $\mathscr{U}(I_3, S)$, and the contribution due to shear deformations $\mathscr{W}(I_1, I_2, I_3, S)$. Thus

$$\mathscr{E}(I_1, I_2, I_3, S) = \mathscr{U}(I_3, S) + \mathscr{W}(I_1, I_2, I_3, S). \tag{55}$$

where I_1, I_2, I_3 denote the invariants of the chosen strain tensor (see § 2). For all testcases the isotropic hyperelastic equation of state from [24] is used, where

$$\mathscr{U}(I_3, S) = \frac{K_0}{2\alpha^2}(I_3^{\alpha/2} - 1)^2 + c_v T_0 I_3^{\gamma/2}(\exp[S/c_v] - 1), \tag{56}$$

and

$$\mathscr{W}(I_1, I_2, I_3) = \frac{B_0}{2} I_3^{\beta/2}(I_1^2/3 - I_2). \tag{57}$$

Here, the invariants correspond to those of the (symmetric) elastic Finger tensor $G = F^{-T}F^{-1}$. The parameters $K_0 = c_0^2 - (4/3)b_0^2$, $B_0 = b_0^2$ are the squared bulk speed of sound and the squared speed of the shear wave, respectively, c_v is heat capacity at constant volume, α, β, γ are constants characterising nonlinear dependence of sound speeds and temperature on the mass density. Material constants for copper are given in Table 1.

In the examples below, initial value problems are solved in a computational domain $[0 : 1]$. The position of the discontinuity in the initial data [cf. (24)] is $x_0 = 0.5$. Where reference is made to first-order solutions forward Euler time integration is used along with first-order reconstruction.

Table 1: Equation of state parameters

Parameter	Value	Units
ρ_0	8.93	$\mathrm{g\,cm^{-}3}$
c_0	4.6	$\mathrm{km\,s^{-1}}$
c_v	$3.9 \cdot 10^{-4}$	$\mathrm{kJ\,g^{-1}\,K^{-1}}$
T_0	300	K
b_0	2.1	$\mathrm{km\,s^{-1}}$
α	1.0	–
β	3.0	–
γ	2.0	–

5.1. Testcase 1

The first testcase considered is similar to the five wave example in [24]. In the present case an additional degree of shear deformation is added so as to study the full seven wave structure. The initial conditions are

$$U_L \left\{ u = \begin{pmatrix} 0 \\ 0.5 \\ 1 \end{pmatrix} \mathrm{km\,s^{-1}},\ F = \begin{pmatrix} 0.98 & 0 & 0 \\ 0.02 & 1 & 0.1 \\ 0 & 0 & 1 \end{pmatrix},\ S = 1 \cdot 10^{-3}\,\mathrm{kJ\,g^{-1}\,K^{-1}} \right.$$

$$U_R \left\{ u = \begin{pmatrix} 0 \\ 0 \\ 0 \end{pmatrix} \mathrm{km\,s^{-1}},\quad F = \begin{pmatrix} 1 & 0 & 0 \\ 0 & 1 & 0.1 \\ 0 & 0 & 1 \end{pmatrix},\quad S = 0\,\mathrm{kJ\,g^{-1}\,K^{-1}} \right.$$

The solution comprises three left travelling rarefaction waves, a right travelling contact, and two right travelling rarefactions led by a right travelling shock wave.

Figure 2 shows various state profiles obtained using the MPWENO-5 scheme with CFL=0.6 and 500 grid points and at time $t = 0.6\,\mu$s. The results are quite satisfactory with no significant over- or under-shoots. The MPWENO-5 scheme was chosen because for this testcase it provided the best tradeoff between cost and resolution. Figure 3 shows density profiles using the first order scheme, WENO-3, MPWENO-5 and MPWENO-9 schemes. As expected WENO-3 and MPWENO-5 offer significant improvements on the first order method. Indeed the small amplitude second transverse waves on both sides of the contact are indistinguishable using first-order. While the MPWENO-9 scheme improves further the resolution of shock and contact waves, undershoots at the foot of rarefaction waves become amplified. Relative CPU-times are given in Table 2.

5.2. Testcase 2

The second testcase is based upon that in [15]. In the original case the initial disturbance causes almost unnoticeable jumps in some parameters across certain transverse waves. It was found that these jumps can

Table 2: Computation times for testcase 1. Times correspond to total CPU time required to reach a solution time $t = 0.6\,\mu$s, with CFL=0.6 for WENO and 0.9 for first order. All times are standardised against first order results.

	1^{st}-order	WENO-3	MPWENO-5	MPWENO-9
CPU Time	1	4.2	5.2	7.2

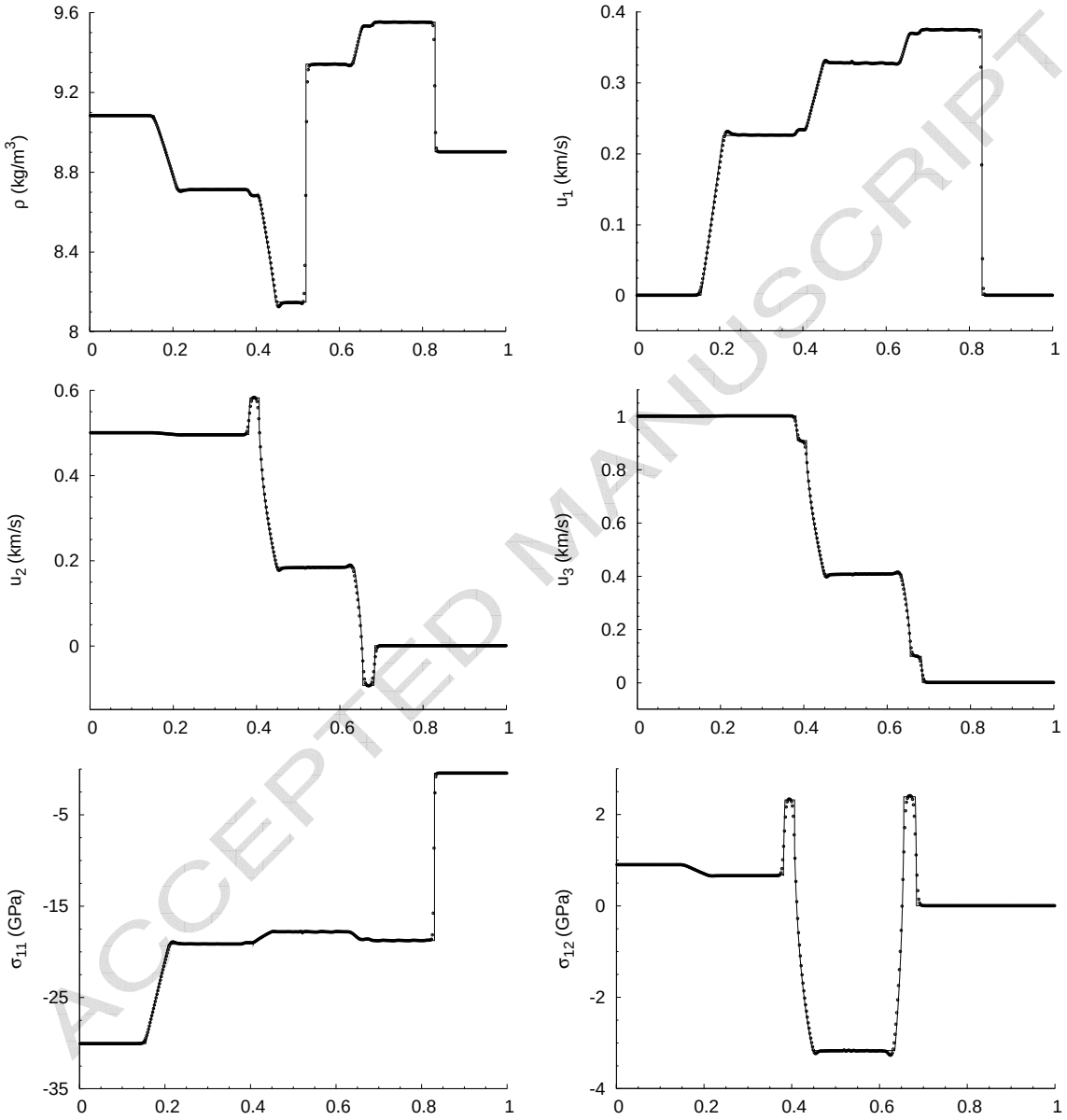

Figure 2: Comparison of exact (solid line) and numerical (points) solutions of Testcase 1 at a time $t = 0.6\,\mu s$. Numerical solutions were obtained with a grid spacing $\Delta x = 1/500$, CFL=0.6, and using the MPWENO 5th.

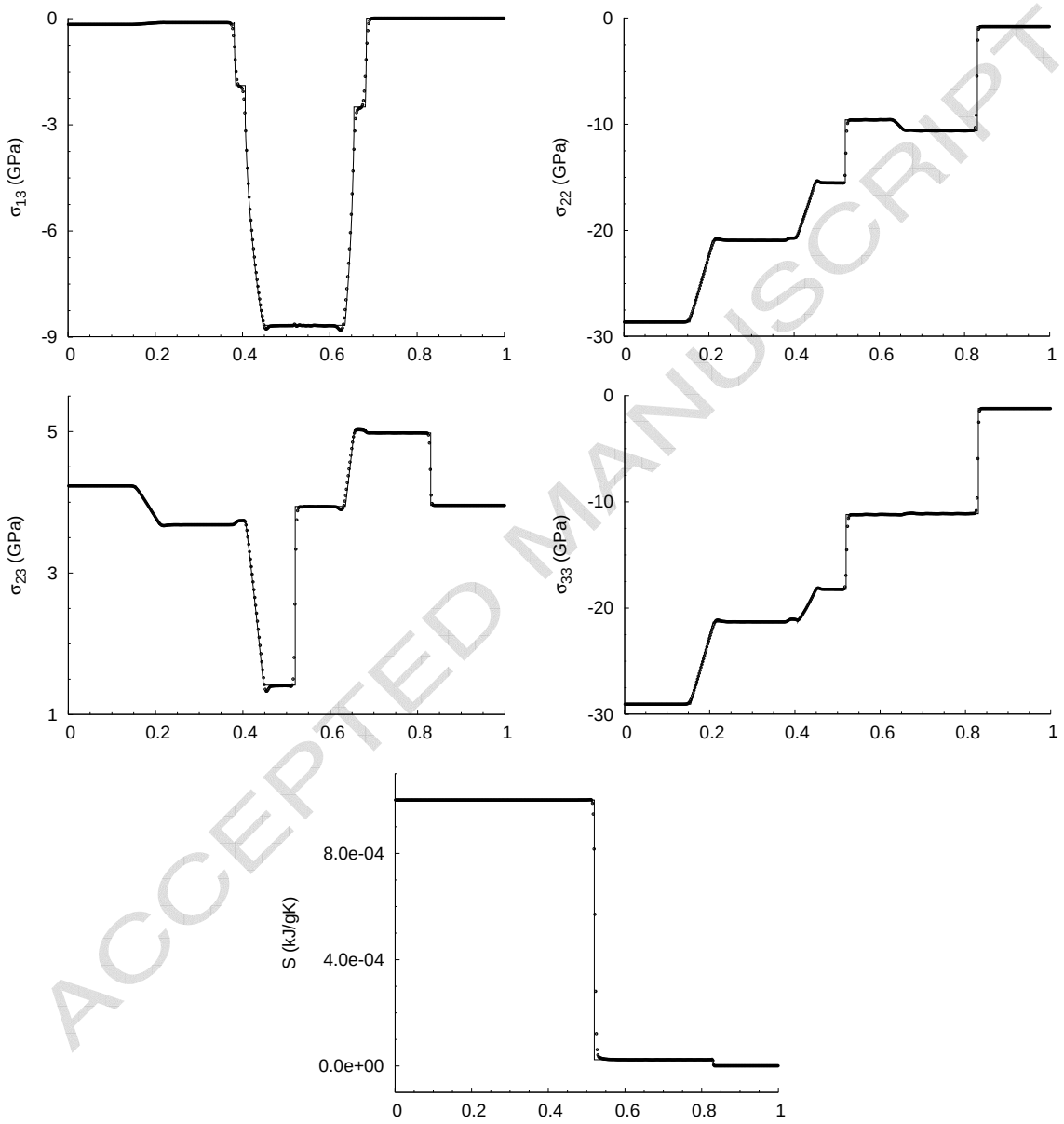

Figure 2: *(continued)*

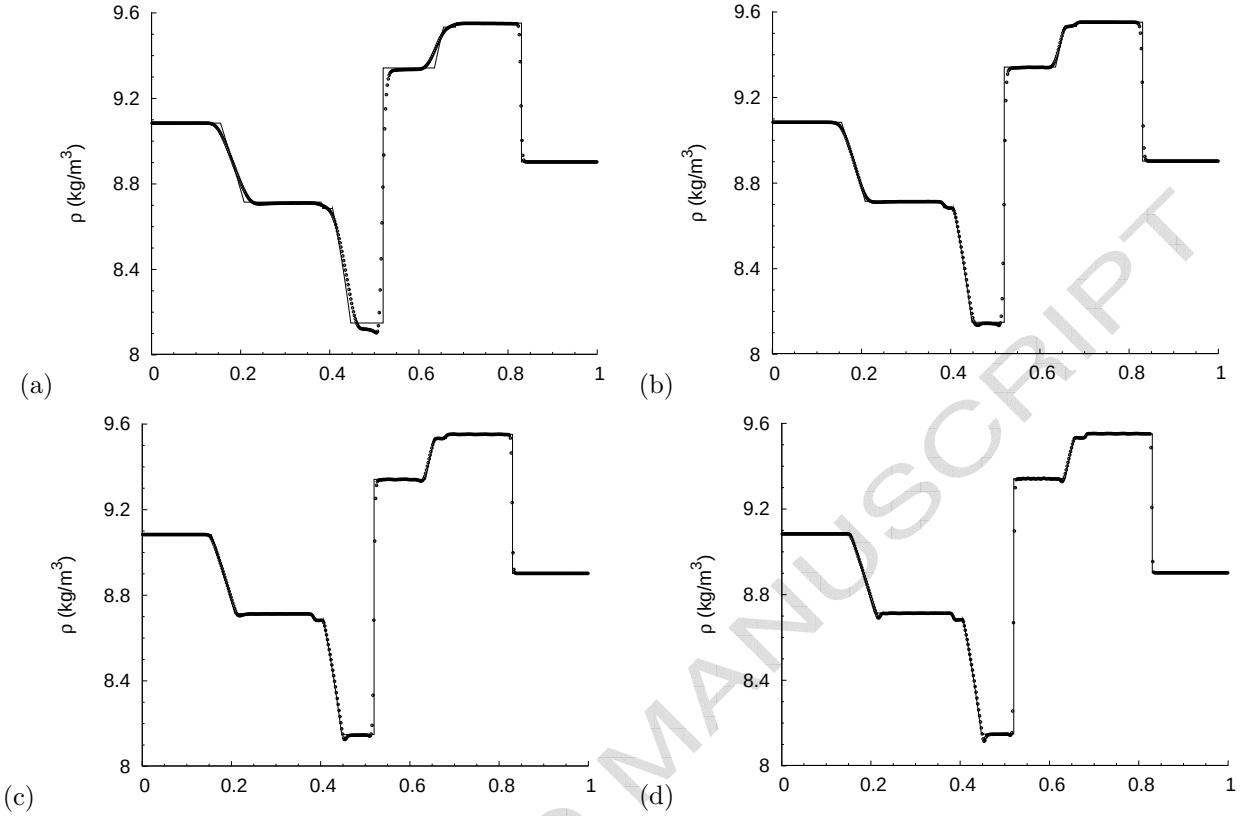

Figure 3: Comparison of exact (solid line) and numerical (points) solutions of Testcase 1 at a time $t = 0.6\,\mu s$. Numerical solutions were obtained with a grid spacing $\Delta x = 1/500$; (a) first-order space and time with CFL=0.9; (b) WENO-3, (c) MPWENO-5, (d) MPWENO-9, all with CFL=0.6.

be amplified by using one additional degree of shear deformation. The initial conditions are

$$U_L \left\{ \begin{array}{l} u = \begin{pmatrix} 2 \\ 0 \\ 0.1 \end{pmatrix} \text{km s}^{-1}, \quad F = \begin{pmatrix} 1 & 0 & 0 \\ -0.01 & 0.95 & 0.02 \\ -0.015 & 0 & 0.9 \end{pmatrix}, \quad S = 0\,\text{kJ g}^{-1}\,\text{K}^{-1} \end{array} \right.$$

$$U_R \left\{ \begin{array}{l} u = \begin{pmatrix} 0 \\ -0.03 \\ -0.01 \end{pmatrix} \text{km s}^{-1}, \quad F = \begin{pmatrix} 1 & 0 & 0 \\ 0.015 & 0.95 & 0 \\ -0.01 & 0 & 0.9 \end{pmatrix}, \quad S = 0\,\text{kJ g}^{-1}\,\text{K}^{-1} \end{array} \right.$$

The solution comprises symmetric left and right travelling wavetypes about the contact wave: a longitudinal shock followed by a tranverse rarefaction and a transverse shock. The central contact propagates to the right.

Results were again obtained using MPWENO-5, with CFL=0.6 and 500 grid points, and run to a time $t = 0.6\,\mu$s. Spurious overshoots occur in those parameters not conserved across the contact wave (Figure 4). This behaviour was observed in [24] for similarly predominantly impact based testcases and is accountable to the Riemann solver. All waves and constant states are distinguishable using MPWENO-5 reconstruction and 500 grid points. It can be shown that the solution converges with decreasing grid spacing (Figure 5).

Resolution of the first shocks and following rarefactions are good on both left and right sides of the contact. However, the slow transverse shocks are captured within quite a few more cells than the longitudinal shocks. This has also been observed for slow moving shocks in magnetohydrodynamics by Balsara et al. [1], where they show that the resolution can be improved using MPWENO-9. While similar improvements can be obtained in non-linear elasticity (Figure 6) it is found that using MPWENO-9 with CFL=0.6 gives rise

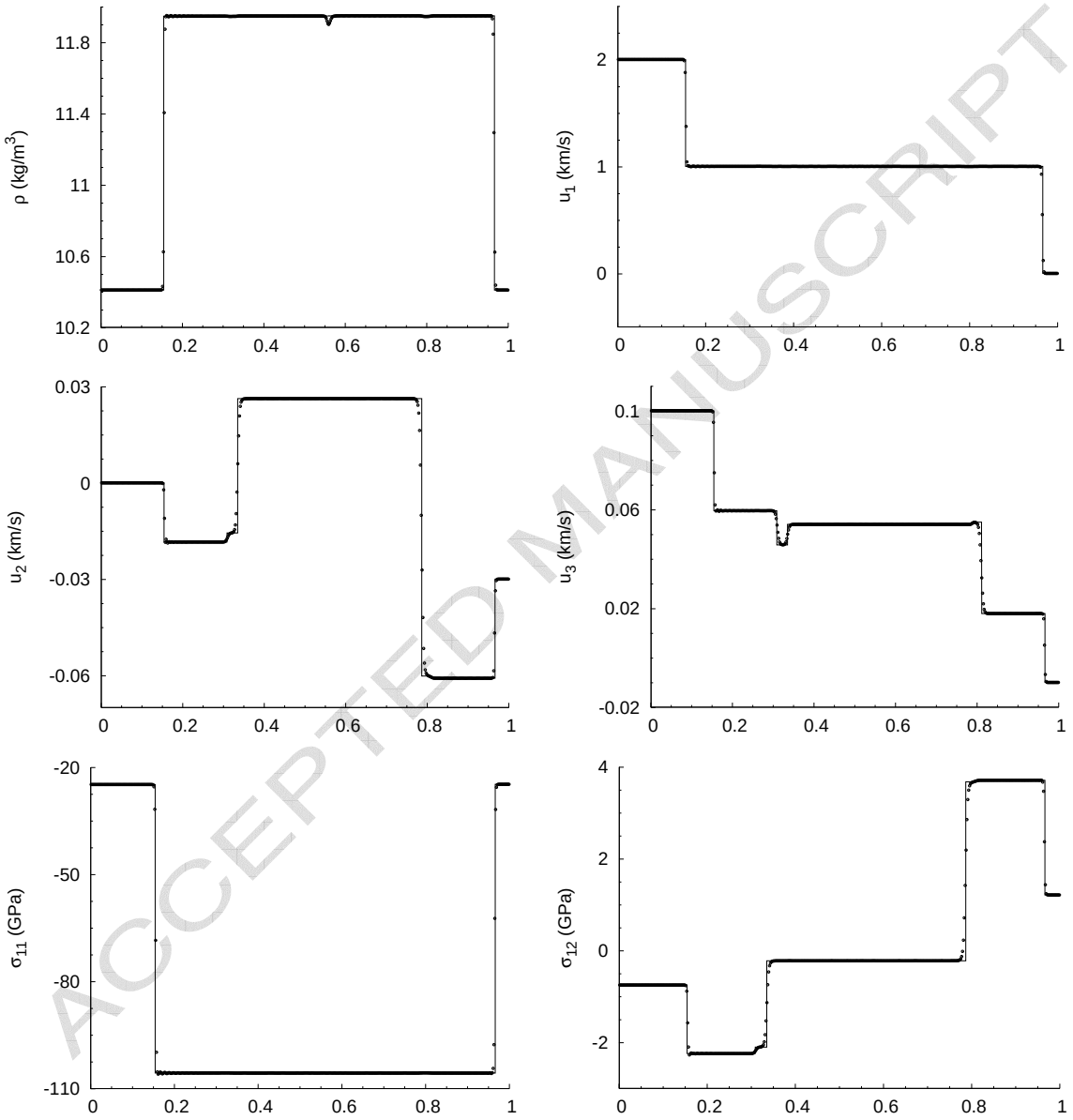

Figure 4: Comparison of exact (solid line) and numerical (points) solutions of Testcase 2 at time $t = 0.6\mu s$. Numerical solutions were obtained with a grid spacing $\Delta x = 1/500$, CFL=0.6, and using the 5th order WENO reconstruction scheme.

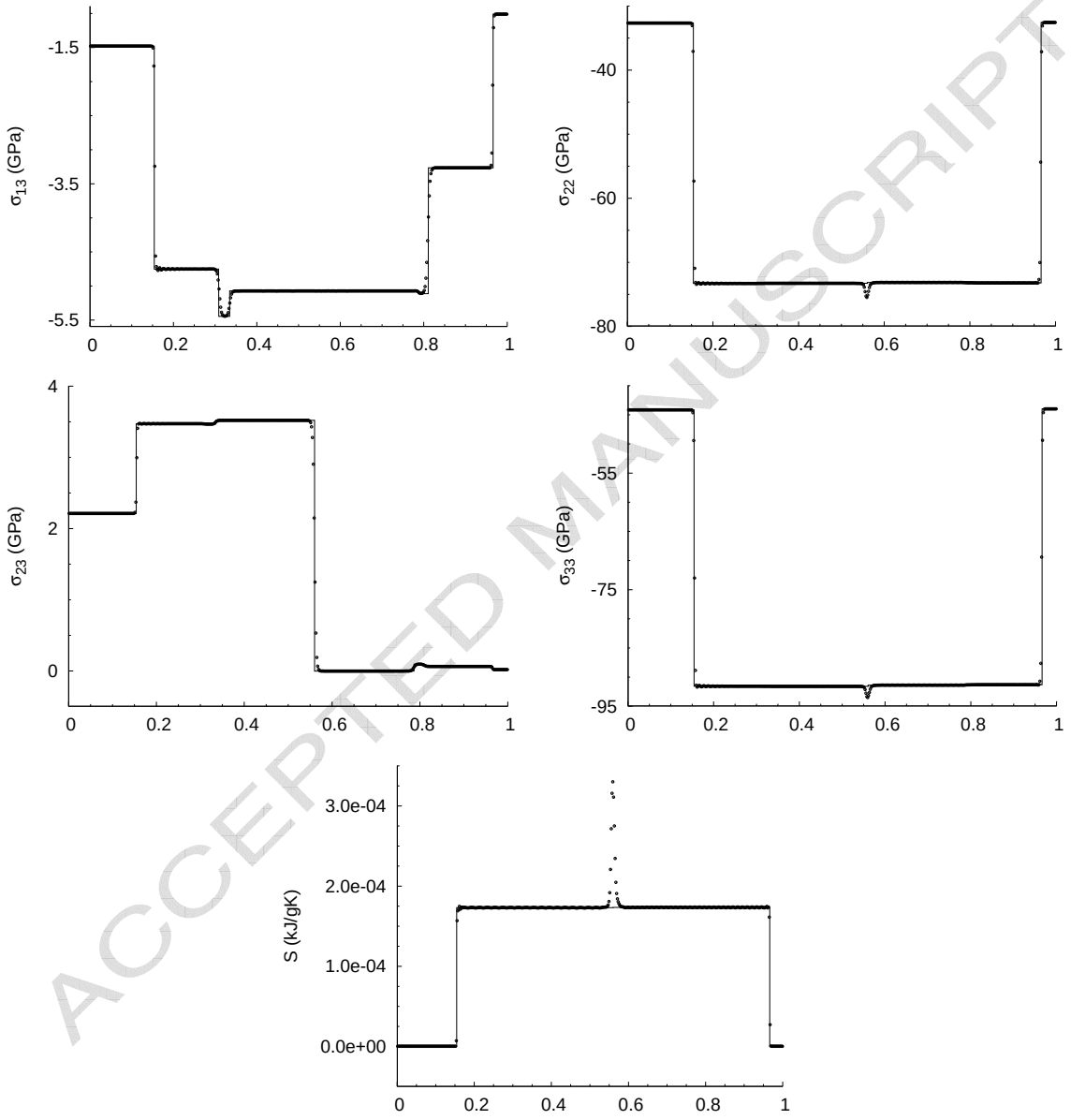

Figure 4: *(continued)*

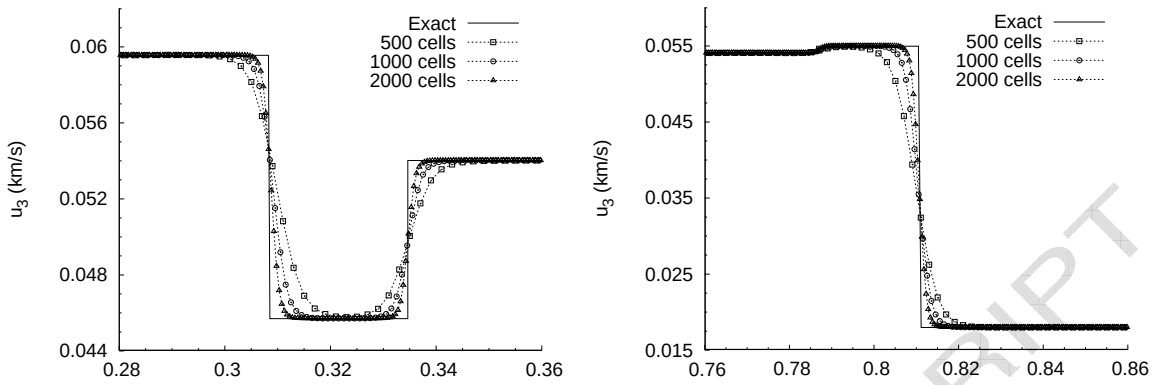

Figure 5: Comparison of exact and numerical solutions of Testcase 2 at a time $t = 0.6\,\mu s$ for different grid spacings. As before: CFL=0.6, and using the 5th order WENO reconstruction scheme.

to oscillatory behaviour in the entropy profile. Instead, using CFL=1/3 dampens almost all of these but doubles the overall cost (CPU-times for Testcase 2 were comparable to those shown in Table 2 for Testcase 1).

6. Summary and Conclusions

The purpose of the present study was to apply existing high–order shock capturing methods to the governing theory of non-linear elasticity with three-dimensional deformations. Specifically, a characteristic based approximation of the Riemann problem was proposed, with high–order spatial accuracy achieved using MPWENO reconstruction and local characteristic decomposition. The methods were developed on the basis of the augmented one-dimensional system of equations and are easily extendable to multi-dimensions and have implications for more complex problems involving material plasticity. Associated compatibility constraints for the augmented system are exactly satisfied regardless of numerical error but may need special attention in multi-dimensional simulations and require further investigation.

The focus has been on using MPWENO schemes to resolve to a high degree structures where all seven waves are distinct in initial value problems. For this, exact solutions proved invaluable and were found using a proposed exact solver. Implementation of the exact solution method is relatively straightforward and although not entirely general has provided sufficient tests to draw the following conclusions

- Excellent agreement is achieved between numerical and exact results
- The close proximity of transverse waves makes jumps in some properties indistinguishable using first order methods. High order WENO and MPWENO resolve these well, even using WENO-3.
- Results using high order methods are essentially non-oscillatory. Spurious overshoots occur in the vicinity of contact waves for variables not conserved across linearly degenerate fields. These are apparent even with first order methods and remains to be improved.
- The increase in computational cost between first order and WENO-3 with three step time integration is quite significant. However, high-order schemes can be used to obtain the accuracy required at lower spatial resolution compared to lower order methods, thereby resulting in reduction of computational cost. This remains to be further demonstrated through application to multi-dimensional problems.
- MPWENO-5 offers the best tradeoff between accuracy and cost. Ninth order reconstruction lends further improvement in resolving slow moving shock waves, which are captured in more cells than longitudinal shocks, but requires lower CFL numbers to achieve monotonic solutions.

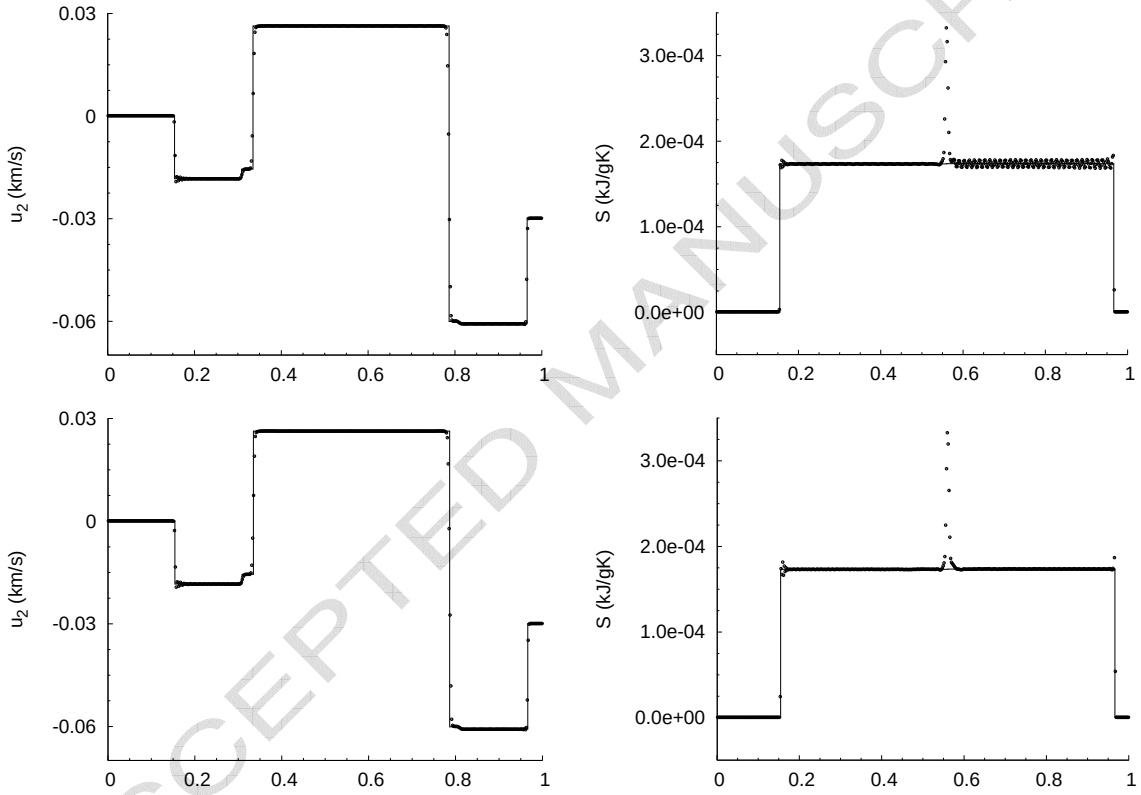

Figure 6: Comparison of exact (solid line) and numerical (points) solutions of Testcase 2 at a time $t = 0.6\,\mu s$, with a grid spacing $\Delta x = 1/500$, using the 9th order WENO reconstruction scheme, with CFL=0.6 (top) and CFL=1/3 (bottom).

Acknowledgements: The financial support from the Engineering and Physical Sciences Research Council (EP/D051940/1) and the MoD-AWE Joint Grant Scheme (JGS 607) is greatly appreciated.

A. Vector and tensor notation

Here some of the vector and tensor notation used throughout this paper is elaborated on. Unless specified otherwise all indices, using for example i, are assumed to range $i = 1, 2, 3$. The following examples are provided for clarity:

- Assume two vectors a and b then

$$a \otimes b^T = \begin{pmatrix} a_1b_1 & a_1b_2 & a_1b_3 \\ a_2b_1 & a_2b_2 & a_2b_3 \\ a_3b_1 & a_3b_2 & a_3b_3 \end{pmatrix},$$

$$a_ib_i = a_1b_1 + a_2b_2 + a_3b_3.$$

- Assume two three-by-three matrices A and B, then

$$A_{ik}B_{kj} = A_{i1}B_{1j} + A_{i2}B_{2j} + A_{i3}B_{3j},$$

$$\sum_{i,j=1}^{3} A_{ij}B_{ij} = A_{11}B_{11} + A_{12}B_{12} + A_{13}B_{13} + \ldots + A_{33}B_{33}.$$

B. Expanded theory

Here, the expanded matrices of eigenvectors are presented, along with a more detailed description of the required coefficients. Expanded, the governing system can be written

$$\frac{\partial}{\partial t}\begin{pmatrix} \rho u_1 \\ \rho u_2 \\ \rho u_3 \\ \rho F_{11} \\ \rho F_{12} \\ \rho F_{13} \\ \rho F_{21} \\ \rho F_{22} \\ \rho F_{23} \\ \rho F_{31} \\ \rho F_{32} \\ \rho F_{33} \\ \rho E \end{pmatrix} + \frac{\partial}{\partial x}\begin{pmatrix} \rho u_1u_1 - \sigma_{11} \\ \rho u_2u_1 - \sigma_{12} \\ \rho u_3u_1 - \sigma_{13} \\ 0 \\ 0 \\ 0 \\ \rho F_{21}u_1 - \rho F_{11}u_2 \\ \rho F_{22}u_1 - \rho F_{12}u_2 \\ \rho F_{23}u_1 - \rho F_{13}u_2 \\ \rho F_{31}u_1 - \rho F_{11}u_3 \\ \rho F_{32}u_1 - \rho F_{12}u_3 \\ \rho F_{33}u_1 - \rho F_{13}u_3 \\ \rho u_1E - u_1\sigma_{11} - u_2\sigma_{12} - u_2\sigma_{13} \end{pmatrix} = 0, \tag{58}$$

with $E = \mathscr{E} + (u_1^2 + u_2^2 + u_3^2)/2$. The left eigenvectors can be written is matrix form as

$$L = (l_1,\, l_2,\, l_3,\, l_4,\, l_5,\, l_6,\, l_7,\, l_8,\, l_9,\, l_{10},\, l_{11},\, l_{12},\, l_{13})^T, \tag{59}$$

where

$$\begin{aligned} l_1 =& ((DQ)_{11},\, (DQ)_{12},\, (DQ)_{13},\, Q_{1i}A^{11}_{i1},\, Q_{1i}A^{11}_{i2},\, Q_{1i}A^{11}_{i3}, \\ & Q_{1i}A^{12}_{i1},\, Q_{1i}A^{12}_{i2},\, Q_{1i}A^{12}_{i3},\, Q_{1i}A^{13}_{i1},\, Q_{1i}A^{13}_{i2},\, Q_{1i}A^{13}_{i3},\, Q_{1i}B^1_i), \\ l_2 =& ((DQ)_{21},\, (DQ)_{22},\, (DQ)_{23},\, Q_{2i}A^{11}_{i1},\, Q_{2i}A^{11}_{i2},\, Q_{2i}A^{11}_{i3}, \\ & Q_{2i}A^{12}_{i1},\, Q_{2i}A^{12}_{i2},\, Q_{2i}A^{12}_{i3},\, Q_{2i}A^{13}_{i1},\, Q_{2i}A^{13}_{i2},\, Q_{2i}A^{13}_{i3},\, Q_{2i}B^1_i), \end{aligned}$$

$$
\begin{aligned}
l_3 =&((DQ)_{31},\ (DQ)_{32},\ (DQ)_{33},\ Q_{3i}A^{11}_{i1},\ Q_{3i}A^{11}_{i2},\ Q_{3i}A^{11}_{i3},\\
&Q_{3i}A^{12}_{i1},\ Q_{3i}A^{12}_{i2},\ Q_{3i}A^{12}_{i3},\ Q_{3i}A^{13}_{i1},\ Q_{3i}A^{13}_{i2},\ Q_{3i}A^{13}_{i3},\ Q_{3i}B^{1}_{i}),\\
l_4 =&(0,\ 0,\ 0,\ F_{12}/F_{11},\ -1,\ 0,\ 0,\ 0,\ 0,\ 0,\ 0,\ 0,\ 0),\\
l_5 =&(0,\ 0,\ 0,\ F_{13}/F_{11},\ 0,\ -1,\ 0,\ 0,\ 0,\ 0,\ 0,\ 0,\ 0),\\
l_6 =&(0,\ 0,\ 0,\ 0,\ 0,\ 0,\ F_{12}/F_{11},\ -1,\ 0,\ 0,\ 0,\ 0,\ 0),\\
l_7 =&(0,\ 0,\ 0,\ 0,\ 0,\ 0,\ F_{13}/F_{11},\ 0,\ -1,\ 0,\ 0,\ 0,\ 0),\\
l_8 =&(0,\ 0,\ 0,\ 0,\ 0,\ 0,\ 0,\ 0,\ 0,\ 0,\ F_{12}/F_{11},\ -1,\ 0,\ 0),\\
l_9 =&(0,\ 0,\ 0,\ 0,\ 0,\ 0,\ 0,\ 0,\ 0,\ 0,\ F_{13}/F_{11},\ 0,\ -1,\ 0),\\
l_{10} =&(0,\ 0,\ 0,\ 0,\ 0,\ 0,\ 0,\ 0,\ 0,\ 0,\ 0,\ 0,\ 0,\ 1),\\
l_{11} =&((DQ)_{31},\ (DQ)_{32},\ (DQ)_{33},\ -Q_{3i}A^{11}_{i1},\ -Q_{3i}A^{11}_{i2},\ -Q_{3i}A^{11}_{i3},\\
&-Q_{3i}A^{12}_{i1},\ -Q_{3i}A^{12}_{i2},\ -Q_{3i}A^{12}_{i3},\ -Q_{3i}A^{13}_{i1},\ -Q_{3i}A^{13}_{i2},\ -Q_{3i}A^{13}_{i3},\ -Q_{3i}B^{1}_{i}),\\
l_{12} =&((DQ)_{21},\ (DQ)_{22},\ (DQ)_{23},\ -Q_{2i}A^{11}_{i1},\ -Q_{2i}A^{11}_{i2},\ -Q_{2i}A^{11}_{i3},\\
&-Q_{2i}A^{12}_{i1},\ -Q_{2i}A^{12}_{i2},\ -Q_{2i}A^{12}_{i3},\ -Q_{2i}A^{13}_{i1},\ -Q_{2i}A^{13}_{i2},\ -Q_{2i}A^{13}_{i3},\ -Q_{2i}B^{1}_{i}),\\
l_{13} =&((DQ)_{11},\ (DQ)_{12},\ (DQ)_{13},\ -Q_{1i}A^{11}_{i1},\ -Q_{1i}A^{11}_{i2},\ -Q_{1i}A^{11}_{i3},\\
&-Q_{1i}A^{12}_{i1},\ -Q_{1i}A^{12}_{i2},\ -Q_{1i}A^{12}_{i3},\ -Q_{1i}A^{13}_{i1},\ -Q_{1i}A^{13}_{i2},\ -Q_{1i}A^{13}_{i3},\ -Q_{1i}B^{1}_{i}).
\end{aligned}
$$

In a similar fashion the right eigenvectors can be written

$$R = (r_1,\ r_2,\ r_3,\ r_4,\ r_5,\ r_6,\ r_7,\ r_8,\ r_9,\ r_{10},\ r_{11},\ r_{12},\ r_{13}), \tag{60}$$

where

$$
\begin{aligned}
r_1 =&\tfrac{1}{2}((Q^{-1}D^{-1})_{11},\ (Q^{-1}D^{-1})_{21},\ (Q^{-1}D^{-1})_{31},\ F_{11}(Q^{-1}D^{-2})_{11},\ F_{12}(Q^{-1}D^{-2})_{11},\\
&F_{13}(Q^{-1}D^{-2})_{11},\ F_{11}(Q^{-1}D^{-2})_{21},\ F_{12}(Q^{-1}D^{-2})_{21},\ F_{13}(Q^{-1}D^{-2})_{21},\\
&F_{11}(Q^{-1}D^{-2})_{31},\ F_{12}(Q^{-1}D^{-2})_{31},\ F_{13}(Q^{-1}D^{-2})_{31},\ 0)^T,\\
r_2 =&\tfrac{1}{2}((Q^{-1}D^{-1})_{12},\ (Q^{-1}D^{-1})_{22},\ (Q^{-1}D^{-1})_{32},\ F_{11}(Q^{-1}D^{-2})_{12},\ F_{12}(Q^{-1}D^{-2})_{12},\\
&F_{13}(Q^{-1}D^{-2})_{12},\ F_{11}(Q^{-1}D^{-2})_{22},\ F_{12}(Q^{-1}D^{-2})_{22},\ F_{13}(Q^{-1}D^{-2})_{22},\\
&F_{11}(Q^{-1}D^{-2})_{32},\ F_{12}(Q^{-1}D^{-2})_{32},\ F_{13}(Q^{-1}D^{-2})_{32},\ 0)^T,\\
r_3 =&\tfrac{1}{2}((Q^{-1}D^{-1})_{13},\ (Q^{-1}D^{-1})_{23},\ (Q^{-1}D^{-1})_{33},\ F_{11}(Q^{-1}D^{-2})_{13},\ F_{12}(Q^{-1}D^{-2})_{13},\\
&F_{13}(Q^{-1}D^{-2})_{13},\ F_{11}(Q^{-1}D^{-2})_{23},\ F_{12}(Q^{-1}D^{-2})_{23},\ F_{13}(Q^{-1}D^{-2})_{23},\\
&F_{11}(Q^{-1}D^{-2})_{33},\ F_{12}(Q^{-1}D^{-2})_{33},\ F_{13}(Q^{-1}D^{-2})_{33},\ 0)^T,\\
r_4 =&(0,\ 0,\ 0,\ F_{11}\Omega^{-1}_{1i}A^{11}_{i2},\ F_{12}\Omega^{-1}_{1i}A^{11}_{i2}-1,\ F_{13}\Omega^{-1}_{1i}A^{11}_{i2},\ F_{11}\Omega^{-1}_{2i}A^{11}_{i2}\\
&F_{12}\Omega^{-1}_{2i}A^{11}_{i2},\ F_{13}\Omega^{-1}_{2i}A^{11}_{i2},\ F_{11}\Omega^{-1}_{3i}A^{11}_{i2},\ F_{12}\Omega^{-1}_{3i}A^{11}_{i2},\ F_{13}\Omega^{-1}_{3i}A^{11}_{i2},\ 0)^T,\\
r_5 =&(0,\ 0,\ 0,\ F_{11}\Omega^{-1}_{1i}A^{11}_{i3},\ F_{12}\Omega^{-1}_{1i}A^{11}_{i3},\ F_{13}\Omega^{-1}_{1i}A^{11}_{i3}-1,\ F_{11}\Omega^{-1}_{2i}A^{11}_{i3}\\
&F_{12}\Omega^{-1}_{2i}A^{11}_{i3},\ F_{13}\Omega^{-1}_{2i}A^{11}_{i3},\ F_{11}\Omega^{-1}_{3i}A^{11}_{i3},\ F_{12}\Omega^{-1}_{3i}A^{11}_{i3},\ F_{13}\Omega^{-1}_{3i}A^{11}_{i3},\ 0)^T,\\
r_6 =&(0,\ 0,\ 0,\ F_{11}\Omega^{-1}_{1i}A^{12}_{i2},\ F_{12}\Omega^{-1}_{1i}A^{12}_{i2},\ F_{13}\Omega^{-1}_{1i}A^{12}_{i2},\ F_{11}\Omega^{-1}_{2i}A^{12}_{i2}\\
&F_{12}\Omega^{-1}_{2i}A^{12}_{i2}-1,\ F_{13}\Omega^{-1}_{2i}A^{12}_{i2},\ F_{11}\Omega^{-1}_{3i}A^{12}_{i2},\ F_{12}\Omega^{-1}_{3i}A^{12}_{i2},\ F_{13}\Omega^{-1}_{3i}A^{12}_{i2},\ 0)^T,\\
r_7 =&(0,\ 0,\ 0,\ F_{11}\Omega^{-1}_{1i}A^{12}_{i3},\ F_{12}\Omega^{-1}_{1i}A^{12}_{i3},\ F_{13}\Omega^{-1}_{1i}A^{12}_{i3},\ F_{11}\Omega^{-1}_{2i}A^{12}_{i3}\\
&F_{12}\Omega^{-1}_{2i}A^{12}_{i3},\ F_{13}\Omega^{-1}_{2i}A^{12}_{i3}-1,\ F_{11}\Omega^{-1}_{3i}A^{12}_{i3},\ F_{12}\Omega^{-1}_{3i}A^{12}_{i3},\ F_{13}\Omega^{-1}_{3i}A^{12}_{i3},\ 0)^T,\\
r_8 =&(0,\ 0,\ 0,\ F_{11}\Omega^{-1}_{1i}A^{13}_{i2},\ F_{12}\Omega^{-1}_{1i}A^{13}_{i2},\ F_{13}\Omega^{-1}_{1i}A^{13}_{i2},\ F_{11}\Omega^{-1}_{2i}A^{13}_{i2}\\
&F_{12}\Omega^{-1}_{2i}A^{13}_{i2},\ F_{13}\Omega^{-1}_{2i}A^{13}_{i2},\ F_{11}\Omega^{-1}_{3i}A^{13}_{i2},\ F_{12}\Omega^{-1}_{3i}A^{13}_{i2}-1,\ F_{13}\Omega^{-1}_{3i}A^{13}_{i2},\ 0)^T,\\
r_9 =&(0,\ 0,\ 0,\ F_{11}\Omega^{-1}_{1i}A^{13}_{i3},\ F_{12}\Omega^{-1}_{1i}A^{13}_{i3},\ F_{13}\Omega^{-1}_{1i}A^{13}_{i3},\ F_{11}\Omega^{-1}_{2i}A^{13}_{i3}\\
&F_{12}\Omega^{-1}_{2i}A^{13}_{i3},\ F_{13}\Omega^{-1}_{2i}A^{13}_{i3},\ F_{11}\Omega^{-1}_{3i}A^{13}_{i3},\ F_{12}\Omega^{-1}_{3i}A^{13}_{i3},\ F_{13}\Omega^{-1}_{3i}A^{13}_{i3},\ 0)^T,\\
r_{10} =&(0,\ 0,\ 0,\ F_{11}\Omega^{-1}_{1i}B^{1}_{i},\ F_{12}\Omega^{-1}_{1i}B^{1}_{i}-1,\ F_{13}\Omega^{-1}_{1i}B^{1}_{i},\ F_{11}\Omega^{-1}_{2i}B^{1}_{i}\\
&F_{12}\Omega^{-1}_{2i}B^{1}_{i},\ F_{13}\Omega^{-1}_{2i}B^{1}_{i},\ F_{11}\Omega^{-1}_{3i}B^{1}_{i},\ F_{12}\Omega^{-1}_{3i}B^{1}_{i},\ F_{13}\Omega^{-1}_{3i}B^{1}_{i},\ 0)^T,
\end{aligned}
$$

$$
\begin{aligned}
r_{11} =& \tfrac{1}{2}((Q^{-1}D^{-1})_{13},\ (Q^{-1}D^{-1})_{23},\ (Q^{-1}D^{-1})_{33},\ -F_{11}(Q^{-1}D^{-2})_{13},\ -F_{12}(Q^{-1}D^{-2})_{13},\\
& -F_{13}(Q^{-1}D^{-2})_{13},\ -F_{11}(Q^{-1}D^{-2})_{23},\ -F_{12}(Q^{-1}D^{-2})_{23},\ -F_{13}(Q^{-1}D^{-2})_{23},\\
& -F_{11}(Q^{-1}D^{-2})_{33},\ -F_{12}(Q^{-1}D^{-2})_{33},\ -F_{13}(Q^{-1}D^{-2})_{33},\ 0)^T,\\
r_{12} =& \tfrac{1}{2}((Q^{-1}D^{-1})_{12},\ (Q^{-1}D^{-1})_{22},\ (Q^{-1}D^{-1})_{32},\ -F_{11}(Q^{-1}D^{-2})_{12},\ -F_{12}(Q^{-1}D^{-2})_{12},\\
& -F_{13}(Q^{-1}D^{-2})_{12},\ -F_{11}(Q^{-1}D^{-2})_{22},\ -F_{12}(Q^{-1}D^{-2})_{22},\ -F_{13}(Q^{-1}D^{-2})_{22},\\
& -F_{11}(Q^{-1}D^{-2})_{32},\ -F_{12}(Q^{-1}D^{-2})_{32},\ -F_{13}(Q^{-1}D^{-2})_{32},\ 0)^T,\\
r_{13} =& \tfrac{1}{2}((Q^{-1}D^{-1})_{11},\ (Q^{-1}D^{-1})_{21},\ (Q^{-1}D^{-1})_{31},\ -F_{11}(Q^{-1}D^{-2})_{11},\ -F_{12}(Q^{-1}D^{-2})_{11},\\
& -F_{13}(Q^{-1}D^{-2})_{11},\ -F_{11}(Q^{-1}D^{-2})_{21},\ -F_{12}(Q^{-1}D^{-2})_{21},\ -F_{13}(Q^{-1}D^{-2})_{21},\\
& -F_{11}(Q^{-1}D^{-2})_{31},\ -F_{12}(Q^{-1}D^{-2})_{31},\ -F_{13}(Q^{-1}D^{-2})_{31},\ 0)^T.
\end{aligned}
$$

In order to obtain the Riemann invariants as functions of conserved variables it is necessary to have matrices converting partial derivatives of conservative variables to partial derivatives of non-conservative variables, and vice-versa. Putting $C \equiv (\partial W/\partial U)$, then

$$
C = \frac{1}{2\rho}(c_1, c_2, c_3, c_4, c_5, c_6, c_7, c_8, c_9, c_{10}, c_{11}, c_{12}, c_{13}), \tag{61}
$$

where

$$
\begin{aligned}
c_1 =& (2,\ 0\ ,\ 0\ , -u_1F_{11}^{-T}, -u_1F_{12}^{-T}, -u_1F_{13}^{-T}, -u_1F_{21}^{-T}, -u_1F_{22}^{-T},\\
& -u_1F_{23}^{-T}, -u_1F_{31}^{-T}, -u_1F_{32}^{-T}, -u_1F_{33}^{-T},\ 0),\\
c_2 =& (0\ , 2,\ 0\ , -u_2F_{11}^{-T}, -u_2F_{12}^{-T}, -u_2F_{13}^{-T}, -u_2F_{21}^{-T}, -u_2F_{22}^{-T},\\
& -u_2F_{23}^{-T}, -u_2F_{31}^{-T}, -u_2F_{32}^{-T}, -u_2F_{33}^{-T},\ 0),\\
c_3 =& (0\ ,\ 0,\ 2,\ -u_3F_{11}^{-T}, -u_3F_{12}^{-T}, -u_3F_{13}^{-T}, -u_3F_{21}^{-T}, -u_3F_{22}^{-T},\\
& -u_3F_{23}^{-T}, -u_3F_{31}^{-T}, -u_3F_{32}^{-T}, -u_3F_{33}^{-T},\ 0),\\
c_4 =& (0,\ 0,\ 0,\ 2 - F_{11}F_{11}^{-T},\ -F_{11}F_{12}^{-T},\ -F_{11}F_{13}^{-T},\ -F_{11}F_{21}^{-T},\\
& -F_{11}F_{22}^{-T},\ -F_{11}F_{23}^{-T},\ -F_{11}F_{31}^{-T},\ -F_{11}F_{32}^{-T},\ -F_{11}F_{33}^{-T},\ 0),\\
c_5 =& (0,\ 0,\ 0,\ -F_{12}F_{11}^{-T},\ 2 - F_{12}F_{12}^{-T},\ -F_{12}F_{13}^{-T},\ -F_{12}F_{21}^{-T},\\
& -F_{12}F_{22}^{-T},\ -F_{12}F_{23}^{-T},\ -F_{12}F_{31}^{-T},\ -F_{12}F_{32}^{-T},\ -F_{12}F_{33}^{-T},\ 0),\\
c_6 =& (0,\ 0,\ 0,\ -F_{13}F_{11}^{-T},\ -F_{13}F_{12}^{-T},\ 2 - F_{13}F_{13}^{-T},\ -F_{13}F_{21}^{-T},\\
& -F_{13}F_{22}^{-T},\ -F_{13}F_{23}^{-T},\ -F_{13}F_{31}^{-T},\ -F_{13}F_{32}^{-T},\ -F_{13}F_{33}^{-T},\ 0),\\
c_7 =& (0,\ 0,\ 0,\ -F_{21}F_{11}^{-T},\ -F_{21}F_{12}^{-T},\ -F_{21}F_{13}^{-T},\ 2 - F_{21}F_{21}^{-T},\\
& -F_{21}F_{22}^{-T},\ -F_{21}F_{23}^{-T},\ -F_{21}F_{31}^{-T},\ -F_{21}F_{32}^{-T},\ -F_{21}F_{33}^{-T},\ 0),\\
c_8 =& (0,\ 0,\ 0,\ -F_{22}F_{11}^{-T},\ -F_{22}F_{12}^{-T},\ -F_{22}F_{13}^{-T},\ -F_{22}F_{21}^{-T},\\
& 2 - F_{22}F_{22}^{-T},\ -F_{22}F_{23}^{-T},\ -F_{22}F_{31}^{-T},\ -F_{22}F_{32}^{-T},\ -F_{22}F_{33}^{-T},\ 0),\\
c_9 =& (0,\ 0,\ 0,\ -F_{23}F_{11}^{-T},\ -F_{23}F_{12}^{-T},\ -F_{23}F_{13}^{-T},\ -F_{23}F_{21}^{-T},\\
& -F_{23}F_{22}^{-T},\ 2 - F_{23}F_{23}^{-T},\ -F_{23}F_{31}^{-T},\ -F_{23}F_{32}^{-T},\ -F_{23}F_{33}^{-T},\ 0),\\
c_{10} =& (0,\ 0,\ 0,\ -F_{31}F_{11}^{-T},\ -F_{31}F_{12}^{-T},\ -F_{31}F_{13}^{-T},\ -F_{31}F_{21}^{-T},\\
& -F_{31}F_{22}^{-T},\ -F_{31}F_{23}^{-T},\ 2 - F_{31}F_{31}^{-T},\ -F_{31}F_{32}^{-T},\ -F_{31}F_{33}^{-T},\ 0),\\
c_{11} =& (0,\ 0,\ 0,\ 2 - F_{32}F_{11}^{-T},\ -F_{32}F_{12}^{-T},\ -F_{32}F_{13}^{-T},\ -F_{32}F_{21}^{-T},\\
& -F_{32}F_{22}^{-T},\ -F_{32}F_{23}^{-T},\ -F_{32}F_{31}^{-T},\ 2 - F_{32}F_{32}^{-T},\ -F_{32}F_{33}^{-T},\ 0),\\
c_{12} =& (0,\ 0,\ 0,\ -F_{33}F_{11}^{-T},\ -F_{33}F_{12}^{-T},\ -F_{33}F_{13}^{-T},\ -F_{33}F_{21}^{-T},\\
& -F_{33}F_{22}^{-T},\ -F_{33}F_{23}^{-T},\ -F_{33}F_{31}^{-T},\ -F_{33}F_{32}^{-T},\ 2 - F_{33}F_{33}^{-T},\ 0),\\
c_{13} =& (-2\tfrac{\mathrm{d}S}{\mathrm{d}\mathscr{E}}u_1,\ -2\tfrac{\mathrm{d}S}{\mathrm{d}\mathscr{E}}u_2,\ -2\tfrac{\mathrm{d}S}{\mathrm{d}\mathscr{E}}u_3,\ 2\tfrac{\mathrm{d}S}{\mathrm{d}F_{11}} + F_{11}^{-T}T_3,\ 2\tfrac{\mathrm{d}S}{\mathrm{d}F_{12}} + F_{12}^{-T}T_3,\\
& 2\tfrac{\mathrm{d}S}{\mathrm{d}F_{13}} + F_{13}^{-T}T_3,\ 2\tfrac{\mathrm{d}S}{\mathrm{d}F_{21}} + F_{21}^{-T}T_3, 2\tfrac{\mathrm{d}S}{\mathrm{d}F_{22}} + F_{22}^{-T}T_3,\ 2\tfrac{\mathrm{d}S}{\mathrm{d}F_{23}} + F_{23}^{-T}T_3,\\
& 2\tfrac{\mathrm{d}S}{\mathrm{d}F_{31}} + F_{31}^{-T}T_3,\ 2\tfrac{\mathrm{d}S}{\mathrm{d}F_{32}} + F_{32}^{-T}T_3,\ 2\tfrac{\mathrm{d}S}{\mathrm{d}F_{33}} + F_{33}^{-T}T_3,\ 2\tfrac{\mathrm{d}S}{\mathrm{d}\mathscr{E}}).
\end{aligned}
$$

with

$$T_3 = \frac{\mathrm{d}S}{\mathrm{d}\mathscr{E}}(\frac{1}{2}(u_1^2+u_2^2+u_3^2)-\mathscr{E}) - \sum_{i,j=1}^{3}\frac{\mathrm{d}S}{\mathrm{d}F_{ij}}F_{ij}.$$

Similarly the inverse matrix, $C^{-1} \equiv (\partial U/\partial W)$, can be written

$$C^{-1} = \rho(c_1^{-1}, c_2^{-1}, c_3^{-1}, c_4^{-1}, c_5^{-1}, c_6^{-1}, c_7^{-1}, c_8^{-1}, c_9^{-1}, c_{10}^{-1}, c_{11}^{-1}, c_{12}^{-1}, c_{13}^{-1}), \tag{62}$$

where

$$\begin{aligned}
c_1^{-1} =& (1,\ 0\ ,\ 0\ , -u_1F_{11}^{-T}, -u_1F_{12}^{-T}, -u_1F_{13}^{-T}, -u_1F_{21}^{-T}, -u_1F_{22}^{-T},\\
& -u_1F_{23}^{-T}, -u_1F_{31}^{-T}, -u_1F_{32}^{-T}, -u_1F_{33}^{-T},\ 0),\\
c_2^{-1} =& (0\ , 1,\ 0\ , -u_2F_{11}^{-T}, -u_2F_{12}^{-T}, -u_2F_{13}^{-T}, -u_2F_{21}^{-T}, -u_2F_{22}^{-T},\\
& -u_2F_{23}^{-T}, -u_2F_{31}^{-T}, -u_2F_{32}^{-T}, -u_2F_{33}^{-T},\ 0),\\
c_3^{-1} =& (0\ ,\ 0,\ 1,\ -u_3F_{11}^{-T}, -u_3F_{12}^{-T}, -u_3F_{13}^{-T}, -u_3F_{21}^{-T}, -u_3F_{22}^{-T},\\
& -u_3F_{23}^{-T}, -u_3F_{31}^{-T}, -u_3F_{32}^{-T}, -u_3F_{33}^{-T},\ 0),\\
c_4^{-1} =& (0,\ 0,\ 0,\ 1-F_{11}F_{11}^{-T},\ -F_{11}F_{12}^{-T},\ -F_{11}F_{13}^{-T},\ -F_{11}F_{21}^{-T},\\
& -F_{11}F_{22}^{-T},\ -F_{11}F_{23}^{-T},\ -F_{11}F_{31}^{-T},\ -F_{11}F_{32}^{-T},\ -F_{11}F_{33}^{-T},\ 0),\\
c_5^{-1} =& (0,\ 0,\ 0,\ -F_{12}F_{11}^{-T},\ 1-F_{12}F_{12}^{-T},\ -F_{12}F_{13}^{-T},\ -F_{12}F_{21}^{-T},\\
& -F_{12}F_{22}^{-T},\ -F_{12}F_{23}^{-T},\ -F_{12}F_{31}^{-T},\ -F_{12}F_{32}^{-T},\ -F_{12}F_{33}^{-T},\ 0),\\
c_6^{-1} =& (0,\ 0,\ 0,\ -F_{13}F_{11}^{-T},\ -F_{13}F_{12}^{-T},\ 1-F_{13}F_{13}^{-T},\ -F_{13}F_{21}^{-T},\\
& -F_{13}F_{22}^{-T},\ -F_{13}F_{23}^{-T},\ -F_{13}F_{31}^{-T},\ -F_{13}F_{32}^{-T},\ -F_{13}F_{33}^{-T},\ 0),\\
c_7^{-1} =& (0,\ 0,\ 0,\ -F_{21}F_{11}^{-T},\ -F_{21}F_{12}^{-T},\ -F_{21}F_{13}^{-T},\ 1-F_{21}F_{21}^{-T},\\
& -F_{21}F_{22}^{-T},\ -F_{21}F_{23}^{-T},\ -F_{21}F_{31}^{-T},\ -F_{21}F_{32}^{-T},\ -F_{21}F_{33}^{-T},\ 0),\\
c_8^{-1} =& (0,\ 0,\ 0,\ -F_{22}F_{11}^{-T},\ -F_{22}F_{12}^{-T},\ -F_{22}F_{13}^{-T},\ -F_{22}F_{21}^{-T},\\
& 1-F_{22}F_{22}^{-T},\ -F_{22}F_{23}^{-T},\ -F_{22}F_{31}^{-T},\ -F_{22}F_{32}^{-T},\ -F_{22}F_{33}^{-T},\ 0),\\
c_9^{-1} =& (0,\ 0,\ 0,\ -F_{23}F_{11}^{-T},\ -F_{23}F_{12}^{-T},\ -F_{23}F_{13}^{-T},\ -F_{23}F_{21}^{-T},\\
& -F_{23}F_{22}^{-T},\ 1-F_{23}F_{23}^{-T},\ -F_{23}F_{31}^{-T},\ -F_{23}F_{32}^{-T},\ -F_{23}F_{33}^{-T},\ 0),\\
c_{10}^{-1} =& (0,\ 0,\ 0,\ -F_{31}F_{11}^{-T},\ -F_{31}F_{12}^{-T},\ -F_{31}F_{13}^{-T},\ -F_{31}F_{21}^{-T},\\
& -F_{31}F_{22}^{-T},\ -F_{31}F_{23}^{-T},\ 1-F_{31}F_{31}^{-T},\ -F_{31}F_{32}^{-T},\ -F_{31}F_{33}^{-T},\ 0),\\
c_{11}^{-1} =& (0,\ 0,\ 0,\ 2-F_{32}F_{11}^{-T},\ -F_{32}F_{12}^{-T},\ -F_{32}F_{13}^{-T},\ -F_{32}F_{21}^{-T},\\
& -F_{32}F_{22}^{-T},\ -F_{32}F_{23}^{-T},\ -F_{32}F_{31}^{-T},\ 1-F_{32}F_{32}^{-T},\ -F_{32}F_{33}^{-T},\ 0),\\
c_{12}^{-1} =& (0,\ 0,\ 0,\ -F_{33}F_{11}^{-T},\ -F_{33}F_{12}^{-T},\ -F_{33}F_{13}^{-T},\ -F_{33}F_{21}^{-T},\\
& -F_{33}F_{22}^{-T},\ -F_{33}F_{23}^{-T},\ -F_{33}F_{31}^{-T},\ -F_{33}F_{32}^{-T},\ 1-F_{33}F_{33}^{-T},\ 0),\\
c_{13}^{-1} =& (u_1,\ u_2,\ u_3,\ -\tfrac{\mathrm{d}\mathscr{E}}{\mathrm{d}F_{11}}+F_{11}^{-T}E,\ -\tfrac{\mathrm{d}\mathscr{E}}{\mathrm{d}F_{12}}+F_{12}^{-T}E,\ -\tfrac{\mathrm{d}\mathscr{E}}{\mathrm{d}F_{13}}+F_{13}^{-T}E,\\
& -\tfrac{\mathrm{d}\mathscr{E}}{\mathrm{d}F_{21}}+F_{21}^{-T}E,\ -\tfrac{\mathrm{d}\mathscr{E}}{\mathrm{d}F_{22}}+F_{22}^{-T}E,\ -\tfrac{\mathrm{d}\mathscr{E}}{\mathrm{d}F_{23}}+F_{23}^{-T}E,\ -\tfrac{\mathrm{d}\mathscr{E}}{\mathrm{d}F_{31}}+F_{31}^{-T}E,\\
& -\tfrac{\mathrm{d}\mathscr{E}}{\mathrm{d}F_{32}}+F_{32}^{-T}E,\ -\tfrac{\mathrm{d}\mathscr{E}}{\mathrm{d}F_{33}}+F_{33}^{-T}E,\ \tfrac{\mathrm{d}\mathscr{E}}{\mathrm{d}S}).
\end{aligned}$$

The derivatives of entropy in (61), and the derivatives of internal energy density in (62) with respect to deformation gradient can be formulated more easily if they are considered functions of a strain tensor. Rather than consider each separately, it is instead possible to consider the function $\phi = \phi(I_1, I_2, I_3)$, where I_p are the invariants of a chosen strain tensor and a function of deformation, which can represent either internal energy or entropy equations of state. The derivatives can thus be written

$$\frac{\partial\phi}{\partial F_{ij}} = \frac{\mathrm{d}\phi}{\mathrm{d}I_1}\frac{\partial I_1}{\partial F_{ij}} + \frac{\mathrm{d}\phi}{\mathrm{d}I_2}\frac{\partial I_2}{\partial F_{ij}} + \frac{\mathrm{d}\phi}{\mathrm{d}I_3}\frac{\partial I_3}{\partial F_{ij}}. \tag{63}$$

If, for example, the invariants correspond to those of the Finger strain tensor ($G = F^{-T}F^{-1}$), then derivatives of the invariants with respect to deformation can be found as

$$\frac{\mathrm{d}I_1}{\mathrm{d}F_{jm}} = -2G_{jk}F^{-T}_{km}, \qquad \frac{\mathrm{d}I_2}{\mathrm{d}F_{jm}} = -2(G - \mathrm{Tr}(G)I)_{jk}F^{-T}_{km}, \qquad \frac{\mathrm{d}I_3}{\mathrm{d}F_{jm}} = -2I_3F^{-T}_{jm},$$

giving

$$\frac{\partial\phi}{\partial F_{ij}} = -\frac{\mathrm{d}\phi}{\mathrm{d}I_1}\left(2G_{ik}F^{-T}_{kj}\right) - \frac{\mathrm{d}\phi}{\mathrm{d}I_2}\left(2(G - Tr(G)I)_{ik}F^{-T}_{kj}\right) - \frac{\mathrm{d}\phi}{\mathrm{d}I_3}\left(2I_3F^{-T}_{ij}\right). \tag{64}$$

C. Evaluation of the acoustic tensor

In the x_1-direction the acoustic tensor can be written

$$\Omega = \begin{pmatrix} A^{11}_{11}F_{11} + A^{11}_{12}F_{12} + A^{11}_{13}F_{13} & A^{12}_{11}F_{11} + A^{12}_{12}F_{12} + A^{12}_{13}F_{13} & A^{13}_{11}F_{11} + A^{13}_{12}F_{12} + A^{13}_{13}F_{13} \\ A^{11}_{21}F_{11} + A^{11}_{22}F_{12} + A^{11}_{23}F_{13} & A^{12}_{21}F_{11} + A^{12}_{22}F_{12} + A^{12}_{23}F_{13} & A^{13}_{21}F_{11} + A^{13}_{22}F_{12} + A^{13}_{23}F_{13} \\ A^{11}_{31}F_{11} + A^{11}_{32}F_{12} + A^{11}_{33}F_{13} & A^{12}_{31}F_{11} + A^{12}_{32}F_{12} + A^{12}_{33}F_{13} & A^{13}_{31}F_{11} + A^{13}_{32}F_{12} + A^{13}_{33}F_{13} \end{pmatrix}.$$

The acoustic tensor, its eigensystem and the coefficients $A^{ij}_{km} = \partial\sigma_{ik}/\partial F_{jm}$ appear in the eigenvalues and both the left- and right-eigenvectors. It is desirable therefore to evaluate the coefficients A^{ij}_{km} analytically. Computing the required derivatives of stress with respect to deformation for the coefficients is lengthy, but when decomposed become more approachable. To begin with it is intuitive to elaborate on the definition of the stress tensor. For an isotropic hyperelastic material the internal energy density can be formulated in terms of the invariants of any chosen strain tensor, I_p, with $p = 1, 2, 3$: $\mathscr{E} = \mathscr{E}(I_1, I_2, I_3, S)$. Thus it is more convenient to formulate stress in terms of the strain tensor, instead of the deformation gradient tensor. Taking as an example the Elastic Finger tensor, $G = F^{-T}F^{-1}$, then stress is given by Eq. (8). Formulations of stress in terms of alternative strain tensors commonly employed in solid mechanics can be found in [8]. Using this definition of the equation of state the components of stress can be formulated in terms of density, the derivatives of internal energy density with respect to the invariants of strain, and the components of the strain tensor G,

$$\sigma_{ij} = -2\rho G_{ik}\left(\mathscr{E}_{I_1}\frac{\partial I_1}{\partial G_{jk}} + \mathscr{E}_{I_2}\frac{\partial I_2}{\partial G_{jk}} + \mathscr{E}_{I_3}\frac{\partial I_3}{\partial G_{jk}}\right), \tag{65}$$

where $\mathscr{E}_{I_p} = \partial\mathscr{E}/\partial I_p$ denotes derivatives of internal energy density with respect to the invariants I_p, which will of course depend on the specific formulation of the equation of state. The derivatives of the invariants with respect to the components of the strain tensor can be found as [8]

$$\frac{\mathrm{d}I_1}{\mathrm{d}G_{jk}} = \delta_{jk}, \qquad \frac{\mathrm{d}I_2}{\mathrm{d}G_{jk}} = I_1\delta_{jk} - G_{jk}, \qquad \frac{\mathrm{d}I_3}{\mathrm{d}G_{jk}} = I_3G^{-1}_{jk}.$$

where δ_{jk} is the Kronecker delta. Using these results, the stress tensor can be expressed as a function of ρ, G and $\mathscr{E}_{I_p}$. Thus, the coefficients can be written

$$A^{ij}_{km} = \frac{\mathrm{d}\sigma_{ik}}{\mathrm{d}\rho}\frac{\partial\rho}{\partial F_{jm}} + \left(\sum_{q,r=1}^{3}\frac{\mathrm{d}\sigma_{ik}}{\mathrm{d}G_{qr}}\frac{\partial G_{qr}}{\partial F_{jm}}\right) + \frac{\mathrm{d}\sigma_{ik}}{\mathrm{d}\mathscr{E}_{I_1}}\frac{\partial\mathscr{E}_{I_1}}{\partial F_{jm}} + \frac{\mathrm{d}\sigma_{ik}}{\mathrm{d}\mathscr{E}_{I_2}}\frac{\partial\mathscr{E}_{I_2}}{\partial F_{jm}} + \frac{\mathrm{d}\sigma_{ik}}{\mathrm{d}\mathscr{E}_{I_3}}\frac{\partial\mathscr{E}_{I_3}}{\partial F_{jm}}. \tag{66}$$

The derivatives in the first term in Eq. (66) are $\mathrm{d}\sigma_{ik}/\mathrm{d}\rho = \sigma_{ik}/\rho$ and

$$\frac{\partial\rho}{\partial F} = \frac{\rho_0}{\det|F|^2}\begin{pmatrix} F_{23}F_{32} - F_{22}F_{33} & F_{21}F_{33} - F_{23}F_{31} & F_{22}F_{31} - F_{21}F_{32} \\ F_{12}F_{33} - F_{13}F_{32} & F_{13}F_{31} - F_{11}F_{33} & F_{11}F_{32} - F_{12}F_{31} \\ F_{13}F_{22} - F_{12}F_{23} & F_{11}F_{23} - F_{13}F_{21} & F_{12}F_{21} - F_{11}F_{22} \end{pmatrix}.$$

The large number of derivatives of strain with respect to deformation in the second term in Eq. (66) can be found using any symbolic mathematics package. Since the stress tensor is symmetric it is necessary only

to define the derivatives of six components of stress with respect to strain. Derivatives of σ_{11} with respect to G:

$$\frac{\partial\sigma_{11}}{\partial G_{11}} = -2\rho(\frac{\partial\mathscr{E}}{\partial I_1} + (G_{22}+G_{33})\frac{\partial\mathscr{E}}{\partial I_2} + (-G_{23}G_{32}+G_{22}G_{33})\frac{\partial\mathscr{E}}{\partial I_3}),$$
$$\frac{\partial\sigma_{11}}{\partial G_{12}} = 2\rho(G_{21}\frac{\partial\mathscr{E}}{\partial I_2} - (G_{23}G_{31}-G_{21}G_{33})\frac{\partial\mathscr{E}}{\partial I_3}),\quad \frac{\partial\sigma_{11}}{\partial G_{13}} = 2\rho(G_{31}\frac{\partial\mathscr{E}}{\partial I_2} - (-G_{22}G_{31}+G_{21}G_{32})\frac{\partial\mathscr{E}}{\partial I_3}),$$
$$\frac{\partial\sigma_{11}}{\partial G_{21}} = 2\rho(G_{12}\frac{\partial\mathscr{E}}{\partial I_2} - (G_{13}G_{32}-G_{12}G_{33})\frac{\partial\mathscr{E}}{\partial I_3}),\quad \frac{\partial\sigma_{11}}{\partial G_{22}} = -2\rho(G_{11}\frac{\partial\mathscr{E}}{\partial I_2} + (-G_{13}G_{31}+G_{11}G_{33})\frac{\partial\mathscr{E}}{\partial I_3}),$$
$$\frac{\partial\sigma_{11}}{\partial G_{23}} = -2\rho(G_{12}G_{31}-G_{11}G_{32})\frac{\partial\mathscr{E}}{\partial I_3},\quad \frac{\partial\sigma_{11}}{\partial G_{31}} = 2\rho(G_{13}\frac{\partial\mathscr{E}}{\partial I_2} - (-G_{13}G_{22}+G_{12}G_{23})\frac{\partial\mathscr{E}}{\partial I_3})$$
$$\frac{\partial\sigma_{11}}{\partial G_{32}} = -2\rho(G_{13}G_{21}-G_{11}G_{23})\frac{\partial\mathscr{E}}{\partial I_3},\quad \frac{\partial\sigma_{11}}{\partial G_{33}} = -2\rho(G_{11}\frac{\partial\mathscr{E}}{\partial I_2} + (-G_{12}G_{21}+G_{11}G_{22})\frac{\partial\mathscr{E}}{\partial I_3}).$$

Derivatives of σ_{12} with respect to G:

$$\frac{\partial\sigma_{12}}{\partial G_{11}} = 0,\quad \frac{\partial\sigma_{12}}{\partial G_{12}} = -2\rho(\frac{\partial\mathscr{E}}{\partial I_1} + G_{33}\frac{\partial\mathscr{E}}{\partial I_2}),\quad \frac{\partial\sigma_{12}}{\partial G_{13}} = 2\rho G_{32}\frac{\partial\mathscr{E}}{\partial I_2},\quad \frac{\partial\sigma_{12}}{\partial G_{21}} = 0,\quad \frac{\partial\sigma_{12}}{\partial G_{22}} = 0,$$
$$\frac{\partial\sigma_{12}}{\partial G_{23}} = 0,\quad \frac{\partial\sigma_{12}}{\partial G_{31}} = 0,\quad \frac{\partial\sigma_{12}}{\partial G_{32}} = 2\rho G_{13}\frac{\partial\mathscr{E}}{\partial I_2},\quad \frac{\partial\sigma_{12}}{\partial G_{33}} = -2\rho G_{12}\frac{\partial\mathscr{E}}{\partial I_2}.$$

Derivatives of σ_{13} with respect to G:

$$\frac{\partial\sigma_{13}}{\partial G_{11}} = 0,\quad \frac{\partial\sigma_{13}}{\partial G_{12}} = 2\rho G_{23}\frac{\partial\mathscr{E}}{\partial I_2},\quad \frac{\partial\sigma_{13}}{\partial G_{13}} = -2\rho(\frac{\partial\mathscr{E}}{\partial I_1} + G_{22}\frac{\partial\mathscr{E}}{\partial I_2}),\quad \frac{\partial\sigma_{13}}{\partial G_{21}} = 0,$$
$$\frac{\partial\sigma_{13}}{\partial G_{22}} = -2\rho G_{13}\frac{\partial\mathscr{E}}{\partial I_2},\quad \frac{\partial\sigma_{13}}{\partial G_{23}} = 2\rho G_{12}\frac{\partial\mathscr{E}}{\partial I_2},\quad \frac{\partial\sigma_{13}}{\partial G_{31}} = 0,\quad \frac{\partial\sigma_{13}}{\partial G_{32}} = 0,\quad \frac{\partial\sigma_{13}}{\partial G_{33}} = 0.$$

Derivatives of σ_{22} with respect to G:

$$\frac{\partial\sigma_{22}}{\partial G_{11}} = -2\rho(G_{22}\frac{\partial\mathscr{E}}{\partial I_2} + (-G_{23}G_{32}+G_{22}G_{33})\frac{\partial\mathscr{E}}{\partial I_3}),\quad \frac{\partial\sigma_{22}}{\partial G_{12}} = 2\rho(G_{21}\frac{\partial\mathscr{E}}{\partial I_2} - (G_{23}G_{31}-G_{21}G_{33})\frac{\partial\mathscr{E}}{\partial I_3}),$$
$$\frac{\partial\sigma_{22}}{\partial G_{13}} = -2\rho(-G_{22}G_{31}+G_{21}G_{32})\frac{\partial\mathscr{E}}{\partial I_3},\quad \frac{\partial\sigma_{22}}{\partial G_{21}} = 2\rho(G_{12}\frac{\partial\mathscr{E}}{\partial I_2} - (G_{13}G_{32}-G_{12}G_{33})\frac{\partial\mathscr{E}}{\partial I_3}),$$
$$\frac{\partial\sigma_{22}}{\partial G_{22}} = -2\rho(\frac{\partial\mathscr{E}}{\partial I_1} + (G_{11}+G_{33})\frac{\partial\mathscr{E}}{\partial I_2} + (-G_{13}G_{31}+G_{11}G_{33})\frac{\partial\mathscr{E}}{\partial I_3}),$$
$$\frac{\partial\sigma_{22}}{\partial G_{23}} = 2\rho(G_{32}\frac{\partial\mathscr{E}}{\partial I_2} - dI3dG23\frac{\partial\mathscr{E}}{\partial I_3}),\quad \frac{\partial\sigma_{22}}{\partial G_{31}} = -2\rho(-G_{13}G_{22}+G_{12}G_{23})\frac{\partial\mathscr{E}}{\partial I_3},$$
$$\frac{\partial\sigma_{22}}{\partial G_{32}} = 2\rho(G_{23}\frac{\partial\mathscr{E}}{\partial I_2} - (G_{13}G_{21}-G_{11}G_{23})\frac{\partial\mathscr{E}}{\partial I_3}),\quad \frac{\partial\sigma_{22}}{\partial G_{33}} = -2\rho(G_{22}\frac{\partial\mathscr{E}}{\partial I_2} + (-G_{12}G_{21}+G_{11}G_{22})\frac{\partial\mathscr{E}}{\partial I_3}).$$

Derivatives of σ_{23} with respect to G:

$$\frac{\partial\sigma_{23}}{\partial G_{11}} = -2\rho G_{23}\frac{\partial\mathscr{E}}{\partial I_2},\quad \frac{\partial\sigma_{23}}{\partial G_{12}} = 0,\quad \frac{\partial\sigma_{23}}{\partial G_{13}} = 2\rho G_{21}\frac{\partial\mathscr{E}}{\partial I_2},\quad \frac{\partial\sigma_{23}}{\partial G_{21}} = 2\rho G_{13}\frac{\partial\mathscr{E}}{\partial I_2},$$
$$\frac{\partial\sigma_{23}}{\partial G_{22}} = 0,\quad \frac{\partial\sigma_{23}}{\partial G_{23}} = -2\rho(\frac{\partial\mathscr{E}}{\partial I_1} + G_{11}\frac{\partial\mathscr{E}}{\partial I_2}),\quad \frac{\partial\sigma_{23}}{\partial G_{31}} = 0,\quad \frac{\partial\sigma_{23}}{\partial G_{32}} = 0,\quad \frac{\partial\sigma_{23}}{\partial G_{33}} = 0.$$

Derivatives of σ_{33} with respect to G:

$$\frac{\partial\sigma_{33}}{\partial G_{11}} = -2\rho(G_{33}\frac{\partial\mathscr{E}}{\partial I_2} + (-G_{23}G_{32}+G_{22}G_{33})\frac{\partial\mathscr{E}}{\partial I_3}),\quad \frac{\partial\sigma_{33}}{\partial G_{12}} = -2\rho(G_{23}G_{31}-G_{21}G_{33})\frac{\partial\mathscr{E}}{\partial I_3},$$
$$\frac{\partial\sigma_{33}}{\partial G_{13}} = 2\rho(G_{31}\frac{\partial\mathscr{E}}{\partial I_2} - (-G_{22}G_{31}+G_{21}G_{32})\frac{\partial\mathscr{E}}{\partial I_3}),\quad \frac{\partial\sigma_{33}}{\partial G_{21}} = -2\rho(G_{13}G_{32}-G_{12}G_{33})\frac{\partial\mathscr{E}}{\partial I_3},$$
$$\frac{\partial\sigma_{33}}{\partial G_{22}} = -2\rho(G_{33}\frac{\partial\mathscr{E}}{\partial I_2} + (-G_{13}G_{31}+G_{11}G_{33})\frac{\partial\mathscr{E}}{\partial I_3}),\quad \frac{\partial\sigma_{33}}{\partial G_{23}} = 2\rho(G_{32}\frac{\partial\mathscr{E}}{\partial I_2} - dI3dG23\frac{\partial\mathscr{E}}{\partial I_3}),$$
$$\frac{\partial\sigma_{33}}{\partial G_{31}} = 2\rho(G_{13}\frac{\partial\mathscr{E}}{\partial I_2} - (-G_{13}G_{22}+G_{12}G_{23})\frac{\partial\mathscr{E}}{\partial I_3}),\quad \frac{\partial\sigma_{33}}{\partial G_{32}} = 2\rho(G_{23}\frac{\partial\mathscr{E}}{\partial I_2} - (G_{13}G_{21}-G_{11}G_{23})\frac{\partial\mathscr{E}}{\partial I_3}),$$
$$\frac{\partial\sigma_{33}}{\partial G_{33}} = -2\rho(\frac{\partial\mathscr{E}}{\partial I_1} + (G_{11}+G_{22})\frac{\partial\mathscr{E}}{\partial I_2} + (-G_{12}G_{21}+G_{11}G_{22})\frac{\partial\mathscr{E}}{\partial I_3}).$$

Derivatives of stress in last terms on the right-hand-side of Eq. (66) can be found similarly. Derivatives of stress with respect to the first invariant:

$$\frac{\partial\sigma_{11}}{\partial I_1} = -2\rho G_{11},\quad \frac{\partial\sigma_{12}}{\partial I_1} = -2\rho G_{12},\quad \frac{\partial\sigma_{13}}{\partial I_1} = -2\rho G_{13},\quad \frac{\partial\sigma_{21}}{\partial I_1} = -2\rho G_{21},\quad \frac{\partial\sigma_{22}}{\partial I_1} = -2\rho G_{22},$$
$$\frac{\partial\sigma_{23}}{\partial I_1} = -2\rho G_{23},\quad \frac{\partial\sigma_{31}}{\partial I_1} = -2\rho G_{31},\quad \frac{\partial\sigma_{32}}{\partial I_1} = -2\rho G_{32},\quad \frac{\partial\sigma_{33}}{\partial I_1} = -2\rho G_{33}. \tag{67}$$

Derivatives of stress with respect to the second invariant:

$$\frac{\partial\sigma_{11}}{\partial I_2} = -2\rho(G_{11}G_{22}+G_{11}G_{33}-G_{12}G_{21}-G_{13}G_{31}),\quad \frac{\partial\sigma_{12}}{\partial I_2} = -2\rho(G_{12}G_{33}-G_{13}G_{32}),$$
$$\frac{\partial\sigma_{13}}{\partial I_2} = -2\rho(G_{13}G_{22}-G_{12}G_{23}),\quad \frac{\partial\sigma_{21}}{\partial I_2} = -2\rho(G_{21}G_{33}-G_{23}G_{31}),$$
$$\frac{\partial\sigma_{22}}{\partial I_2} = -2\rho(G_{11}G_{22}+G_{22}G_{33}-G_{12}G_{21}-G_{23}G_{32}),\quad \frac{\partial\sigma_{23}}{\partial I_2} = -2\rho(G_{11}G_{23}-G_{13}G_{21}),$$
$$\frac{\partial\sigma_{31}}{\partial I_2} = -2\rho(G_{22}G_{31}-G_{21}G_{32}),\quad \frac{\partial\sigma_{32}}{\partial I_2} = -2\rho(G_{11}G_{32}-G_{12}G_{31}),$$
$$\frac{\partial\sigma_{33}}{\partial I_2} = -2\rho(G_{11}G_{33}+G_{22}G_{33}-G_{13}G_{31}-G_{23}G_{32}).$$

Derivatives of stress with respect to the third invariant:

$$\frac{\partial\sigma_{11}}{\partial I_3} = -2\rho I_3, \quad \frac{\partial\sigma_{22}}{\partial I_3} = -2\rho I_3, \quad \frac{\partial\sigma_{33}}{\partial I_3} = -2\rho I_3,$$
$$\frac{\partial\sigma_{12}}{\partial I_3} = \frac{\partial\sigma_{13}}{\partial I_3} = \frac{\partial\sigma_{21}}{\partial I_3} = \frac{\partial\sigma_{23}}{\partial I_3} = \frac{\partial\sigma_{31}}{\partial I_3} = \frac{\partial\sigma_{32}}{\partial I_3} = 0.$$

The additional derivatives in the last term of Eq. (66) can be decomposed further using

$$\frac{\partial\mathscr{E}_{I_p}}{\partial F_{jm}} = \frac{\mathrm{d}\mathscr{E}_{I_p}}{\mathrm{d}I_1}\frac{\partial I_1}{\partial F_{jm}} + \frac{\mathrm{d}\mathscr{E}_{I_p}}{\mathrm{d}I_2}\frac{\partial I_2}{\partial F_{jm}} + \frac{\mathrm{d}\mathscr{E}_{I_p}}{\mathrm{d}I_3}\frac{\partial I_3}{\partial F_{jm}}. \tag{68}$$

Derivatives of the invariants of the elastic Finger tensor with respect to deformation can be found as

$$\frac{\mathrm{d}I_1}{\mathrm{d}F_{jm}} = -2G_{jk}F^{-T}_{km}, \qquad \frac{\mathrm{d}I_2}{\mathrm{d}F_{jm}} = -2(G - \mathrm{Tr}(G)I)_{jk}F^{-T}_{km}, \qquad \frac{\mathrm{d}I_3}{\mathrm{d}F_{jm}} = -2I_3F^{-T}_{jm}.$$

giving

$$\frac{\partial\mathscr{E}_{I_p}}{\partial F_{jm}} = -\frac{\mathrm{d}\mathscr{E}_{I_p}}{\mathrm{d}I_1}\left(2G_{jk}F^{-T}_{km}\right) - \frac{\mathrm{d}\mathscr{E}_{I_p}}{\mathrm{d}I_2}\left(2(G - \mathrm{Tr}(G)I)_{jk}F^{-T}_{km}\right) - \frac{\mathrm{d}\mathscr{E}_{I_p}}{\mathrm{d}I_3}\left(2I_3F^{-T}_{jm}\right). \tag{69}$$

Depending on the chosen form of the equation of state some of the second derivatives of internal energy density with respect to invariants may be zero.

References

[1] D. S. Balsara and C. Shu, Monotonicity preserving weighted essentially non-oscillatory schemes with increasingly high order accuracy, *J. Comp. Phys.*, **160**, 405 (2000).

[2] D. Drikakis, S. Tsangaris, An Implicit Characteristic Flux Averaging Scheme for the Euler Equations for Real Gases, *International Journal for Numerical Methods in Fluids*, **12**, 711 (1991).

[3] D. Drikakis, P. Govatsos, D. Papantonis, A Characteristic Based Method for Incompressible Flows, *International Journal for Numerical Methods in Fluids*, **19**, 667 (1994).

[4] D. Drikakis and W. Rider, *High-Resolution Methods for Incompressible and Low-Speed Flows*, (Springer, 2005).

[5] A. Eberle, Characteristic Flux Averaging Approach to the Solution of Euler's Equations, in *VKI Lecture Series, Computational Fluid Dynamics* (1987).

[6] X. Garaizar, Solution of a Riemann problem for elasticity, *J. Elasticity*, **26**, 43 (1991).

[7] S. K. Godunov and E. I. Romenskii, Nonstationary Equations of Nonlinear Elasticity Theory in Eulerian Coordinates, *J. App. Mech. Tech. Phys.*, **13**, 868 (1972).

[8] S. K. Godunov and E. I. Romenskii, *Elements of Continuum Mechanics and Conservation Laws*, (Kluwer Academic/Plenum Publishers, 2003).

[9] G. S. Jiang and C. W. Shu, Efficient implementation of weighted ENO schemes, *J. Comp. Phys.*, **126**, 202 (1996).

[10] G. Kluth and B. Després, Perfect plasticity and hyperelastic models for isotropic materials, *Continuum Mech. Thermodyn.*, **20**, 173 (2008).

[11] P. G. LeFloch and F. Olsson, A second-order Godunov method for the conservation laws of nonlinear elastodynamics, *Impact Comp. Sci. Eng*, **2**, 318 (1990).

[12] P. G. LeFloch, Hyperbolic systems of conservation laws: The theory of classical and nonclassical shock waves, (Berkhäuser Varlag, 2002).

[13] G. H. Miller and P. Colella, A High-Order Eulerian Godunov Method for Elastic-Plastic Flow in Solids, *J. Comp. Phys.*, **167**, 131 (2001).

[14] A. Mosedale, D. Drikakis, Assessment of very high-order of accuracy in LES models, *Journal of Fluids Engineering*, **129**, 1497 (2007).

[15] G. H. Miller, An iterative Riemann solver for systems of hyperbolic conservation laws, with application to hyperelastic solid mechanics, *J. Comp. Phys.*, **193**, 198 (2003).

[16] G. H. Miller, Minimal rotationally invariant bases for hyperelasticity, *SIAM J. Appl. Math.*, **64**, 2050 (2004).

[17] B. J. Plohr and D. H. Sharp, A conservative Eulerian formulation of the equations for elastic flow, *Adv. Appl. Math.*, **9**, 418 (1988).

[18] J. Qiu and C. Shu, On the construction, comparison, and local characteristic decomposition for high-order central WENO schemes, *J. Comp. Phys.*, **183**, 187 (2002).

[19] E. I. Romensky, Thermodynamics and Hyperbolic Systems of Balance Laws in Continuum Mechanics, in *Godunov Methods: Theory and Applications*, edited by E. F. Toro (Kluwer Academic/Plenum Publishers, 2001).

[20] E. Shapiro, Step-by-Step Eberle's scheme derivation. Technical report, Cranfield University, (2006).

[21] C. Shu and S. Osher, Efficient Implementation of Essentially Non-oscillatory Shock-Capturing Schemes, *J. Comp. Phys.*, **77**, 439 (1988).

[22] B. T. Smith, B. S. Garbow, J. J. Dongarra, J. M. Boyle and Y. Ikebe, Matrix Eigensystem Routines - EISPACK Guide, 2nd Edition, in *Lecture Notes in Computer Science, Volume 6* (Springer-Verlag, 1976)

[23] B. Thornber, A. Mosedale, D. Drikakis, On the implicit large eddy simulations of homogeneous decaying turbulence, *Journal of Computational Physics*, **226**, 1902 (2007).

[24] V. A. Titarev, E. Romenski and E. F. Toro, MUSTA-type upwind fluxes for non-linear elasticity, *Int. J. Numer. Meth. Eng.*, **73** 897 (2008).

[25] E. F. Toro, Riemann Solvers and Numerical Methods for Fluid Dynamics: A Practical Introduction, 2nd Edition, (Springer, 1999).

[26] J. A. Trangenstein and P. Colella, A Higher-Order Godunov Method for Modelling Finite Deformation in Elastic-Plastic Solids, *Comm. Pure App. Math.*, **44**, 41 (1991).

[27] J. A. Trangenstein and R. B. Pember, Numerical algorithms for strong discontinuities in elastic-plastic solids, *J. Comp. Phys.*, **103**, 63 (1992).

[28] O. Y. Vorobiev, I. N. Lomov, A. V. Shutov, V. I. Kondaurov, A.L. Ni and V. E. Fortov, Application of schemes on moving grids for numerical simulation of hypervelocity impact problems, *Int. J. Impact Eng.*, **17** 891 (1995).

[29] F. Wang, J. G. Glimm, J. W. Grove and B. J. Plohr, A conservative Eulerian numerical scheme for elastoplasticity and application to plate impact problems, *Impact Comp. Sci. Eng.*, **5** 285 (1993).